

For Reference

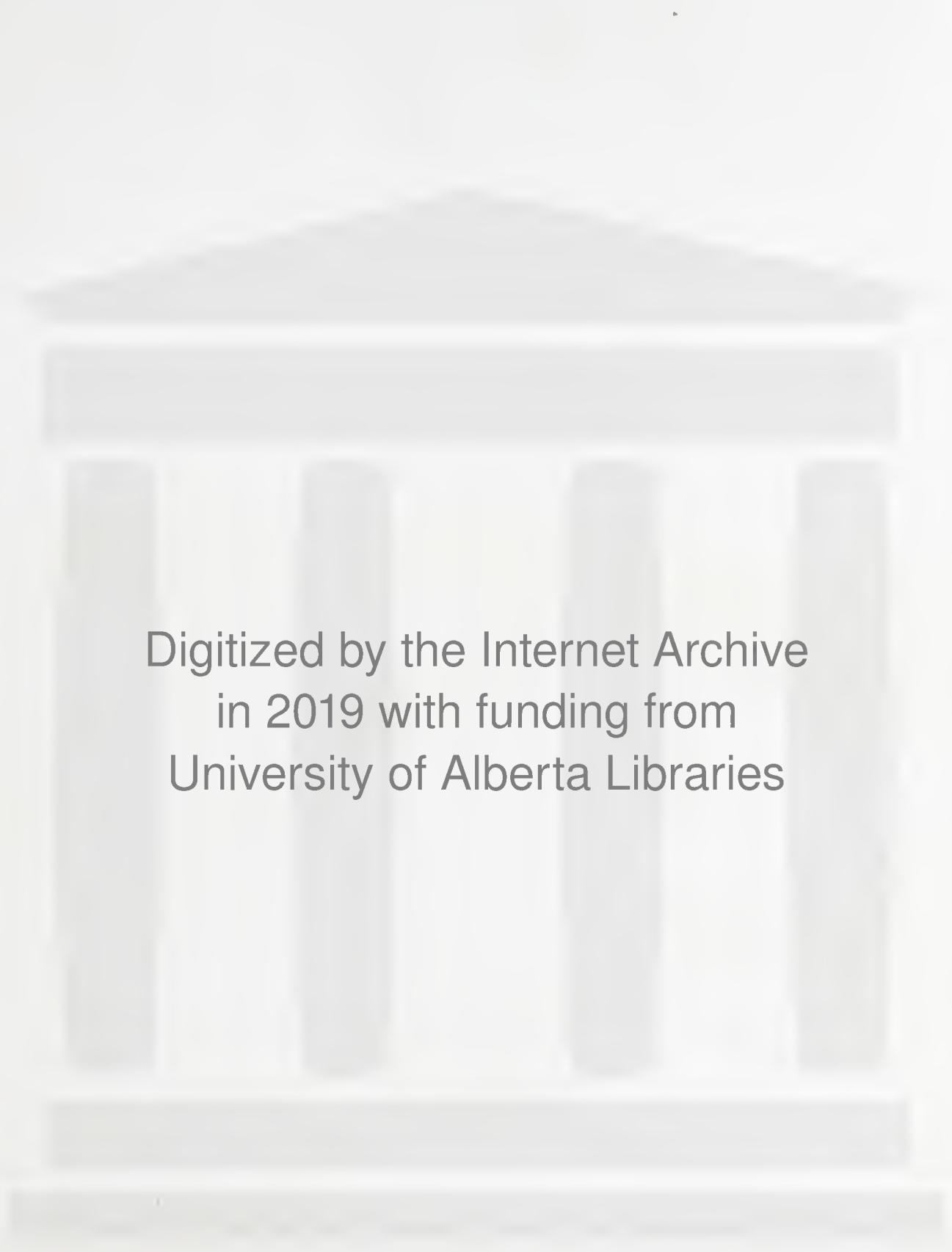
NOT TO BE TAKEN FROM THIS ROOM

For Reference

NOT TO BE TAKEN FROM THIS ROOM

Ex LIBRIS
UNIVERSITATIS
ALBERTAENSIS





Digitized by the Internet Archive
in 2019 with funding from
University of Alberta Libraries

<https://archive.org/details/horizontalannula00kazi>



Thesis
1961
#4

THE UNIVERSITY OF ALBERTA

HORIZONTAL ANNULAR-MIST FLOW OF NATURAL GAS-WATER MIXTURES

A THESIS

SUBMITTED TO THE FACULTY OF GRADUATE STUDIES
IN PARTIAL FULFILMENT OF THE REQUIREMENTS FOR THE DEGREE
OF MASTER OF SCIENCE IN PETROLEUM ENGINEERING

DEPARTMENT OF CHEMICAL AND PETROLEUM ENGINEERING

by

K. AZIZ

EDMONTON, ALBERTA

APRIL 7, 1961

ABSTRACT

A survey of the literature having possible application to the annular-mist flow problem is presented.

The horizontal annular-mist flow of natural gas-water mixtures in one- and two-inch diameter, schedule 40 aluminum pipes was investigated. The input gas-liquid volume ratios were varied between 10 and 100,000 for superficial gas velocities between 25 and 300 ft. per sec. The mid-point pressure was held constant at 120 psig. Some data for variable mid-point pressure and constant liquid and gas rates are also presented to show the effect of gas density.

The pressure drop data for constant mid-point density are presented as a function of the superficial velocities of the two phases. The same data are also presented in terms of the ratio of the two-phase pressure gradient to the single-phase gas pressure gradient. Possible mechanisms of the flow in the annular-mist region are discussed and the possibility of microscopic changes in flow pattern is indicated. A large effect of a small quantity of water was observed over the gas rates investigated. Higher water rates had much greater

effect at low gas rates than at high gas rates. It is proposed that the high pressure drop is caused by the formation of a liquid film on the inside wall of the pipe. The thickness of this film decreases as the gas rate is increased until it reaches some minimum value. The breakup of this film was not indicated over the range of gas rates investigated. A correlation is proposed for low liquid rates based on the data of this investigation.

The data are also interpreted in terms of a friction factor and Reynolds number based on the mixture properties.

ACKNOWLEDGEMENTS

The author wishes to express his gratitude to Dr. G.W. Govier for his guidance and assistance in supervising this investigation.

The author is indebted to the Pan American Petroleum Corporation for the graduate fellowship, the Karachi Gas Company Limited for making it possible to come to Canada for this study and the National Research Council of Canada for financial support.

Sincere thanks are extended to Northwestern Utilities Limited for providing space, natural gas, water, some of the equipment, and the help of their personnel during this investigation. The author also wishes to express his appreciation to Barber Engineering, Canadian Meter Company and Canadian Chemicals for the loan of their equipment.

Acknowledgement is made to Mr. R. Kirby and Mr. H. Tebelmann of the University of Alberta and Mr. D. Cusack of Northwestern Utilities for their assistance during the construction of the equipment; to Mr. R.A.S. Brown for his many helpful suggestions, especially in photographic work.

TABLE OF CONTENTS

	<u>PAGE</u>
List of Tables	i
List of Figures	ii
List of Plates	iv
I Introduction	1
II Literature Review	7
III Experimental Equipment	16
IV Experimental Procedure	28
V Experimental Results	33
VI Discussion of Results	51
VII Conclusions	59
Nomenclature	60
Bibliography	62

Appendices

A Composition of the Gas and Geometry of the System	65
B Experimental and Calculated Data	69
C Calibration Data	113

LIST OF TABLES

<u>TABLE</u>		<u>PAGE</u>
1	Experimental Data Obtained	30
A-1	Composition of the Gas	66
A-2	Summary of Data Describing Test Sections	68
B-1	One-Inch Pipe Experimental Data	70
B-2	Two-Inch Pipe Experimental Data	74
B-3	One-Inch Pipe Calculated Data	80
B-4	Two-Inch Pipe Calculated Data	84
B-5	One-Inch Pipe Pressure Gradient Ratio Data	90
B-6	Two-Inch Pipe Pressure Gradient Ratio Data	94
B-7	One-Inch Pipe Calculated Data Based on Mixture Properties	97
B-8	Two-Inch Pipe Calculated Data Based on Mixture Properties	103

LIST OF FIGURES

<u>FIGURE</u>		<u>PAGE</u>
1	Schematic Equipment Diagram	17
2	Detail of Pipe Joints	19
3	Detail of Pressure Taps	19
4	One-Inch Pipe Pressure Drop Measurement and Pressure Control Equipment	23
5	Two-Inch Pipe Pressure Drop Measurement and Pressure Control Equipment	24
6	Typical One-Inch Pressure Gradient Curves	37
7	One-Inch Pipe Basic Pressure Drop Data for Constant Mid-point Gas Density = 0.47 lbs. per ft. ³ $\frac{dP}{dL}$ versus V_g for Various Constant V_w	38
8	Two-Inch Pipe Basic Pressure Drop Data for Constant Mid-point Gas Density = 0.47 lbs. per ft. ³ $\frac{dP}{dL}$ versus V_g for Various Constant V_w	39
9	One-Inch Pipe Pressure Drop Data for Constant and Mid-point Gas Density = 0.47 lbs. per ft. ³ $\frac{dP}{dL}$ versus $(V_w + .0001)$ for Various Constant V_g	41
10	Two-Inch Pipe Pressure Drop Data for Constant and Mid-point Gas Density = 0.47 lbs. per ft. ³ $\frac{dP}{dL}$ versus $(V_w + .0001)$ for Various Constant V_g	42
11	One-Inch Pipe $(\frac{dP}{dL})/(\frac{dP}{dL})_g$ versus V_g for Various Constant V_w	44

12	Two-Inch Pipe $(\frac{dP}{dL}) / (\frac{dP}{dL})_g$ versus V_g for Various Constant V_w	45
13	One-Inch Pipe Data Based on Mixture Properties f_{tpm} versus Re_m for Various Constant R_v	46
14	Two-Inch Pipe Data Based on Mixture Properties f_{tpm} versus Re_m for Various Constant R_v	47
15	Variable Density Data at Constant Flow Rates $(\frac{dP}{dL}) / (\frac{dP}{dL})_g$ versus ρ_g for Various Flow Rates	48
16	Comparison of the Two-Inch and One-Inch Pipe Data by Eliminating the Diameter and Roughness Effects. The Correlation of the Data for Low Water Flow Rates	54
C-1	Calibration of Water D/P Cell Orifices	117
C-2	One-Inch Pipe Single Phase Gas Flow Data at High Reynolds Numbers	118
C-3	One- and Two-Inch Pipe Single Phase Friction Factor versus Reynolds Number Curves	119

LIST OF PLATES

<u>PLATE</u>		<u>PAGE</u>
I	Transparent Section in One-Inch Pipe	25
II	Instrument Air Supply Air Compressor and Surge Tank	27
III	Photographs of Flow Pattern	50

I INTRODUCTION

The engineer in recent years has encountered many problems concerned with the simultaneous flow of liquids and gases, immiscible liquids, and solids and liquids. The petroleum engineer has been particularly concerned with the simultaneous flow of gases and liquids in the reservoir, well bore, gathering lines, transmission lines and processing plant equipment. A better understanding of the two phase flow in the well bore could allow more accurate prediction of flowing bottom hole pressures. More recently, centrally located batteries in oil fields have resulted in long gathering lines which must be designed for multiphase flow. The design of gas-lift installations could also be greatly improved if the flow pattern and pressure drop could be predicted more accurately.

A considerable amount of work, both theoretically and experimentally, has been done towards a general solution of the problem of gas-liquid flow. Omer (1), Wood (2) and Bennett (3) have presented good literature surveys of the work done on two-phase horizontal and vertical flow.

The problem of interest to the engineer involves the prediction of the pressure drop and sometimes the flow pattern

from the fluid properties and flow rates along with the diameter, length, roughness and orientation of the pipe.

Single-phase Flow

It is instructive to first review briefly the work that has been done on single-phase flow. The Fanning friction factor for flow in circular tubes is defined by the equation

$$f = \frac{g_c D}{2\rho V^2} \frac{dP_f}{dL} \quad (1)$$

where f = Fanning friction factor

$\frac{dP_f}{dL}$ = pressure drop per unit length due to friction alone

V = linear velocity

ρ = fluid density

D = internal pipe diameter

If the extensive available data are interpreted in terms of the friction factor so defined, then for laminar flow

$$f = \frac{16}{Re} \quad (2)$$

where Re = Reynolds number for laminar flow (< 2000).

This result has also been derived theoretically.

From the table following we find the number of
 cases, separately for each of the 10 years.

Year

1. In connection with the cases of the
 year 1900, the number of cases is 100. The number of cases
 in 1901 is 100. The number of cases in 1902 is 100.

$$\frac{100}{100} = 1$$

Year 1903

$$\frac{100}{100} = 1$$

$$\frac{100}{100} = 1$$

$$\frac{100}{100} = 1$$

$$\frac{100}{100} = 1$$

On the whole, the number of cases is 100. The number of cases
 in 1900 is 100. The number of cases in 1901 is 100.

$$\frac{100}{100} = 1$$

On the whole, the number of cases is 100. The number of cases
 in 1900 is 100. The number of cases in 1901 is 100.

On the whole, the number of cases is 100. The number of cases
 in 1900 is 100. The number of cases in 1901 is 100.

For turbulent flow the value of f cannot be predicted from theory alone, but must be determined by actual experimental work. By dimensional analysis it can be shown that, for turbulent flow, the friction factor is a function of the Reynolds number, $\frac{D\rho V}{\mu}$, and of the relative roughness, $\frac{e}{D}$, which is the ratio of absolute roughness to pipe diameter.

Nikuradse (4), by means of his own experimental data and that of other investigators on smooth pipes obtained the following relationship between f and Re :

$$\frac{1}{\sqrt{f}} = 4.0 \log (Re \sqrt{f}) - 0.40 \quad (3)$$

where $Re > 3000$

Von Karman (6), using the universal velocity-distribution, derived a theoretical equation which had the same form as the Nikuradse equation and differed only slightly from it in the value of the constants.

$$\frac{1}{\sqrt{f}} = 4.06 \log (Re \sqrt{f}) - 0.60 \quad (4)$$

The difference between these two equations is small.

The friction factor curves for rough pipes follow the smooth tube friction factor equation for a short range of Reynolds numbers. Beyond this region there is a transition to fully developed turbulent flow.

For the transition region Colebrook (7) proposed the following empirical equation:

$$\frac{1}{\sqrt{f}} = 4 \log \frac{D}{e} + 2.28 - 4 \log \left(1 + 4.67 \frac{D/e}{Re \sqrt{f}} \right) \quad (5)$$

where $\frac{D/e}{Re \sqrt{f}} \leq 0.01$ (6)

At values of $\frac{D/e}{Re \sqrt{f}} > 0.01$ the flow is fully turbulent and the friction factor is then independent of the Reynolds number. Von Karman's theoretical equation for fully developed turbulent flow, based on the universal velocity-distribution, is

$$\frac{1}{\sqrt{f}} = 4 \log \frac{D}{e} + 2.28 \quad (7)$$

Two-phase Flow

In single-phase flow the energy loss resulting from the irreversibilities is due to the viscous effects and eddy dissipation. In the simultaneous flow of immiscible fluids, additional energy loss is caused by the interaction of the fluids. The problem is complicated since there are many flow patterns and experience has shown that the flow pattern has a great effect on the energy loss.

In a horizontal pipe, when the liquid and gas rates are both small, the two phases flow separately, with liquid at the bottom of the pipe, and the flow is called stratified. If

the liquid rate is then held constant and the gas rate is increased, the liquid surface develops waves or ripples. Further increase in the gas rate causes the liquid to climb the pipe wall and to coalesce at the top. This type of flow, which consists of a continuous core of gas surrounded by a layer of liquid adhering to the tube wall, is called annular flow. More rapid gas rates cause a portion of the liquid to be dispersed into the gas stream in the form of mist, reducing the thickness of the liquid film. This type of flow is called annular-mist and is the subject of the present study. Still higher gas rates may cause the liquid film to break up and result in a mist flow. If, in the previously mentioned stratified flow, more liquid were flowing before the gas velocity was increased, the liquid might fill the pipe for short lengths separated by large bubbles of gas. In most cases many small bubbles would be mixed in the liquid. Such a flow is often called slug flow. Still larger gas rates will again cause annular and annular-mist flow as in the previous case. If the liquid and gas rates were increased simultaneously, the flow would probably consist of gas bubbles dispersed throughout the liquid.

Any two phase flow phenomenon is defined uniquely by the physical properties of each phase, the system geometry and the

mass flow rate of each phase. In reviewing the present state of knowledge it is clear that the relationship between the system variables and the energy loss due to irreversibilities is a complicated one. The only hope of solving this problem completely appears to be in treating each flow pattern separately and analyzing the flow mechanism. This point of view is reflected in the recent literature.

The present investigation is concerned with the study of horizontal flow of gas-liquid mixtures at high gas and low liquid rates. In this region, part of the liquid is dispersed (or entrained) in the gas stream and part of it forms an annular film on the inside pipe wall. This type of mist or annular-mist flow is likely to occur in condensate gas fields both in the well bore and the gathering lines when producing at high rates.

II LITERATURE REVIEW

A considerable amount of work has been done, since the 1930's, on the flow of gas liquid mixtures. Not a great deal of this work applies to the mist or annular-mist flow regions and the larger proportion of this relates to vertical flow. As previously mentioned many investigators have presented good general reviews of the subject (1, 2, 3). The present review is restricted to investigations with possible application to the annular-mist flow region.

One of the earlier and still very widely used correlations is that of Lockhart and Martinelli (7). They presented their correlation as a log-log plot of Φ_g and Φ_l versus X with the flow type as parameter, where

$$\Phi_g^2 = \frac{\left(\frac{\Delta P}{\Delta L}\right)}{\left(\frac{\Delta P}{\Delta L}\right)_g} \quad (8)$$

$$\Phi_l^2 = \frac{\left(\frac{\Delta P}{\Delta L}\right)}{\left(\frac{\Delta P}{\Delta L}\right)_l} \quad (9)$$

$$\text{and } X^2 = \frac{\left(\frac{\Delta P}{\Delta L}\right)_l}{\left(\frac{\Delta P}{\Delta L}\right)_g} \quad (10)$$

The correlation was based on data obtained in pipe sizes up to one-inch diameter. The values of X^2 for annular-mist flow are usually below the range investigated by Martinelli (7), necessitating extrapolation of the curves. The application of this correlation in the annular-mist flow region results in calculated pressure drops which are too low (8). In addition the Martinelli parameters have been found inadequate for the correlation of data in the annular-mist flow region (8, 9).

Chenoweth and Martin (9) obtained data of low liquid volume fractions at pressures up to 100 p.s.i.a. in 1 1/2-inch and 3-inch diameter pipes. The deviations of the data from the Lockhart and Martinelli correlation were systematic. A correlation has been presented as a logarithmic plot of $\frac{\Delta P}{\Delta P_1}$ versus liquid volume fraction with a parameter which reduces to $\frac{f_g \rho_l}{f_l \rho_g}$ for straight pipe.

Baker (10, 11) collected field data, some of which approaches the annular-mist region, for gas-oil mixtures in 4- to 10-inch diameter lines. The length of lines varied from 2 to 8 miles. He found Martinelli's correlation to be inadequate and presented equations for each flow regime separately.

These equations employ Martinelli's parameters. No equations were presented for mist or annular-mist flow.

Hoogendoorn (8) obtained limited data in the annular-mist flow regime in 24, 50 and 91 mm. diameter pipes with air and gas-oil (viscosity = 2.36 c.p., S.G. = 0.815), and also in 50 mm. pipe with air and spindle oil (viscosity = 20.8 c.p., S.G. = 0.905). The data for superficial gas Reynolds numbers (Re_g) from 2×10^5 to 6×10^5 and liquid mass velocities from 9.2 to 855 $\frac{\text{lb.}}{\text{ft}^2 \text{ sec.}}$ have been presented as

a plot of the two phase friction factor $f_g = \left[\frac{(\frac{dP}{dL}) \ g_c \ D}{2 \ V_g^2 \ \rho_g} \right]$

based upon gas properties against the superficial gas Reynolds

($Re_g = \frac{D \ \rho_g \ V_g}{\mu_g}$) number with the water rate as parameter.

Over the limited range, Hoogendoorn has found that, for liquid rates which are not too low, the friction factor is independent of the liquid rate. Also no influence of air density on friction factor was observed for air densities between 0.075 and 0.187 $\frac{\text{lbs.}}{\text{ft}^3}$.

Govier, Radford and Dunn (12) analyzed the problem of the isothermal flow of air and water mixtures in vertical tubes and showed from thermodynamic considerations that the total

unit pressure drop could be expressed by the relationships:

$$-v_1 \left(\frac{\Delta P}{\Delta L} \right) = \frac{1 + R_m}{1 + R_v} + \frac{1}{1 + R_v} \frac{2 f'_1 v_1^2}{g_c D} \quad (11)$$

or

$$-v_g \left(\frac{\Delta P}{\Delta L} \right) = \frac{1 + \frac{1}{R_m}}{1 + \frac{1}{R_v}} + \frac{1}{1 + \frac{1}{R_v}} \frac{2 f'_g v_g^2}{g_c D} \quad (12)$$

These equations define a friction factor based upon either the liquid or gas properties as used by Govier and associates. The first term on the right-hand side of the equation is defined as the hydrostatic head component and the second term as the irreversibility component. Actually, however, the first term represents the hydrostatic head only if there is no holdup. Govier included the entire effect of holdup in the second term. It is, therefore, not possible to compare the irreversibility component from this analysis with the energy loss due to irreversibility in horizontal flow.

Bennett and Thornton (13) calculated the friction factor based on liquid properties as defined by Govier et al. The experiments were conducted in vertical glass pipes of 1.36-inch and 1.25-inch internal diameter and also in an

annulus between 1-inch outside diameter and 1.5-inch inside diameter glass pipes. This annular-mist flow data has been graphically represented by two straight lines on a log-log plot where $f_1' \times Re_g$ is plotted against Re_1 . The data for the annulus and the larger pipe are represented by one line and the data for the smaller pipe by the other line. Slopes of these lines are -2.81 and -2.75 respectively.

In a recent study Ros (14) has made use of dimensional analysis to study the simultaneous flow of oil and gas in vertical pipes. He has derived an equation for "mist flow" which is only valid for flow at atmospheric conditions. This type of study shows promise in multiphase flow applications.

Teletov (15) based his correlation on a friction factor and Reynolds number based on the mixture properties which may be represented as

$$f_{tpm} = \frac{g_c D}{2(V_1 + V_g)^2 \rho_m} \frac{dP}{dL} \quad (13)$$

$$Re_m = \frac{D \rho_1 V_1}{\mu_1} + \frac{D \rho_g V_g}{\mu_g} \quad (14)$$

The correlation was presented in terms of a deviation factor, Ψ , as a function of the volume fraction of liquid and the viscosity ratio of the two phases. The deviation factor

is defined as

$$\Psi = \frac{f_{tpm}}{f^*} \quad (15)$$

where

f^* = friction factor at Re_m from single-phase charts or equations.

The object of the correlations of Lockhart and Martinelli (7), Govier et al (12), Bennett and Thornton (13), Chenoweth and Martin (9) and others of this type is to allow the prediction of pressure drop directly from the flow variables without requiring a mechanistic analysis of the flows in the various regions. The total energy dissipation due to irreversibilities is usually expressed in terms of a two-phase friction factor or some other single factor.

For the specific case of annular-mist flow, where measurements of entrainment and film thickness are available, a different type of analysis may be applied. In this type of analysis the flow in the liquid film and that in the gas core with entrained liquid are treated separately to calculate the pressure drop. This general approach has been taken by Wicks and Dukler (16), Calvert and Williams (17), Anderson and Mantzouranis (19) and Collier and Hewitt (20) and McManus (21). An effort has been made by these investigators to understand the flow mechanism by a study of the microscopic nature of the flow pattern.

Wicks and Dukler (16) have reported entrainment data for annular-mist flow of air-water mixtures in one-and three-inch diameter horizontal pipes. The pressure drop data were presented only for the one-inch pipe. Their investigation covered air rates from 125 to 475 lbs./hr. and water rates from 521 to 3126 lbs./hr. The influence of entrance section design on pressure drop and entrainment was demonstrated. A correlation relating an "entrainment variable" to the ratio of the single-phase pressure drop gradients was also presented.

The analyses of Calvert and Mantzouranis were derived for upwards vertical flow. These have been applied to the flow data of Bennett and Thornton and others by Collier.

The object of the analysis of Calvert and Williams (17) was to calculate the liquid flow in an annular film from a knowledge of the film thickness and the pressure drop. This was achieved by postulating a velocity distribution for the film in terms of shear (and thus pressure drop). The film was assumed to consist of a laminar layer adjacent to the wall and a turbulent layer. The velocity distributions for these two layers were integrated with respect to the distance from the wall to yield the total liquid flow rate.

Anderson and Mantzouranis (18, 19) have used the universal velocity profile of von Karman. Integration of this

velocity profile to yield film flow rates from film thickness and pressure drop data might be more accurate than the Calvert derivation since the former takes account of the existence of the "buffer" region between the laminar and turbulent regions.

Collier and Hewitt (20) applied the Mantzouranis and the Calvert analyses to predict the liquid film flow rates. Mantzouranis' analysis predicted the rates more closely than the Calvert analysis. At high gas rates and low liquid rates the predicted film flow rates were much higher than the actual in both the Calvert and Mantzouranis analyses. Two possible reasons for deviation are given:

- (1) Interchange of droplets between the gas core and the liquid film - the resulting acceleration/deceleration effects causing a loss of energy.
- (2) The collapse of surface waves on the liquid film with consequent dissipation of energy.

Since the wave system is maintained this would result in pressure loss. The waves might also have a profound effect on the velocity distribution in the film.

McManus (19) has reported on the local values of film thickness and wave heights in horizontal two-phase flow. He

has shown that appreciable eccentricity of the film exists and that the wave height is exponentially related to the film depth. It has been suggested that these effects must be accounted for in any complete analysis of horizontal flow.




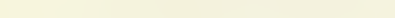
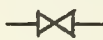
III EXPERIMENTAL EQUIPMENT

The equipment was designed to obtain pressure drop data for a natural gas-water system at high superficial gas velocities (30 to 300 ft/sec.) and low superficial water velocities (0.001 to 1 ft/sec.). The flow control and measurement equipment was selected to give the maximum desired velocities in a one-inch diameter pipe. The range of velocities investigated for the two-inch pipe was lower with the same maximum mass flow rates as in the one-inch pipe.

Arrangements were made with Northwestern Utilities Limited (the natural gas distribution company for the city of Edmonton) to install all equipment at their City Gate Station No. 1. Natural gas at sufficiently high pressure was available at this place.

Two test sections of aluminum schedule 40 pipe having internal diameters of 1.049 and 2.067 inches were installed as shown in Figure 1. The one-inch test section was 40 feet long with approximately 15 feet of calming section upstream and downstream of the test section. Five pressure taps spaced 10 feet apart were provided on the one-inch test section. The two-

KEY TO FIGURE 1

	Gas and Two-phase Lines
	Water Lines
	Instrument Air Lines
	Electrical Lines
	Hand Operated Valves
(1)	Gas Supply Valve
(2)	Mid-point Pressure Control Valve
(3)	Safety Relief Valve
(4)	Electric Heat Exchanger - 8 K.W.
(5)	Electric Heat Exchanger - 3 K.W.
(6)	2-inch Orifice Meter
(7), (8)	Dial Thermometers
(9)	Transparent Section in One-Inch Pipe
(10), (11), (12)	Dial Thermometers
(13)	Hand Operated Back Pressure Control Valve
(14)	Water Pump - 3 H.P.
(15)	Water Pump - 5 H.P.
(16)	Water Rate Control Valve - 1/8 Inch Orifice
(17)	Water Rate Control Valve - 1/2 Inch Orifice
(18)	Integral Orifice D/P Cell
(19)	Mid-point Pressure Transmitter
(20)	Electrical D/P Cell on One-Inch Pipe
(21), (22)	Pneumatic D/P Cell on Two-Inch Pipe
(23)	Mid-point Pressure Recorder and Controller
(24)	Orifice Meter Static and Differential Recorder
(25)	Water Rate Recorder and Controller
(26)	Recorder for Pressure Drop in Two-Inch Pipe
(27)	Multipoint Recorder for Pressure Drop in One-Inch Pipe
(28)	Mercury Manometer for Instrument Calibration
(29)	Water Manometer for Instrument Calibration

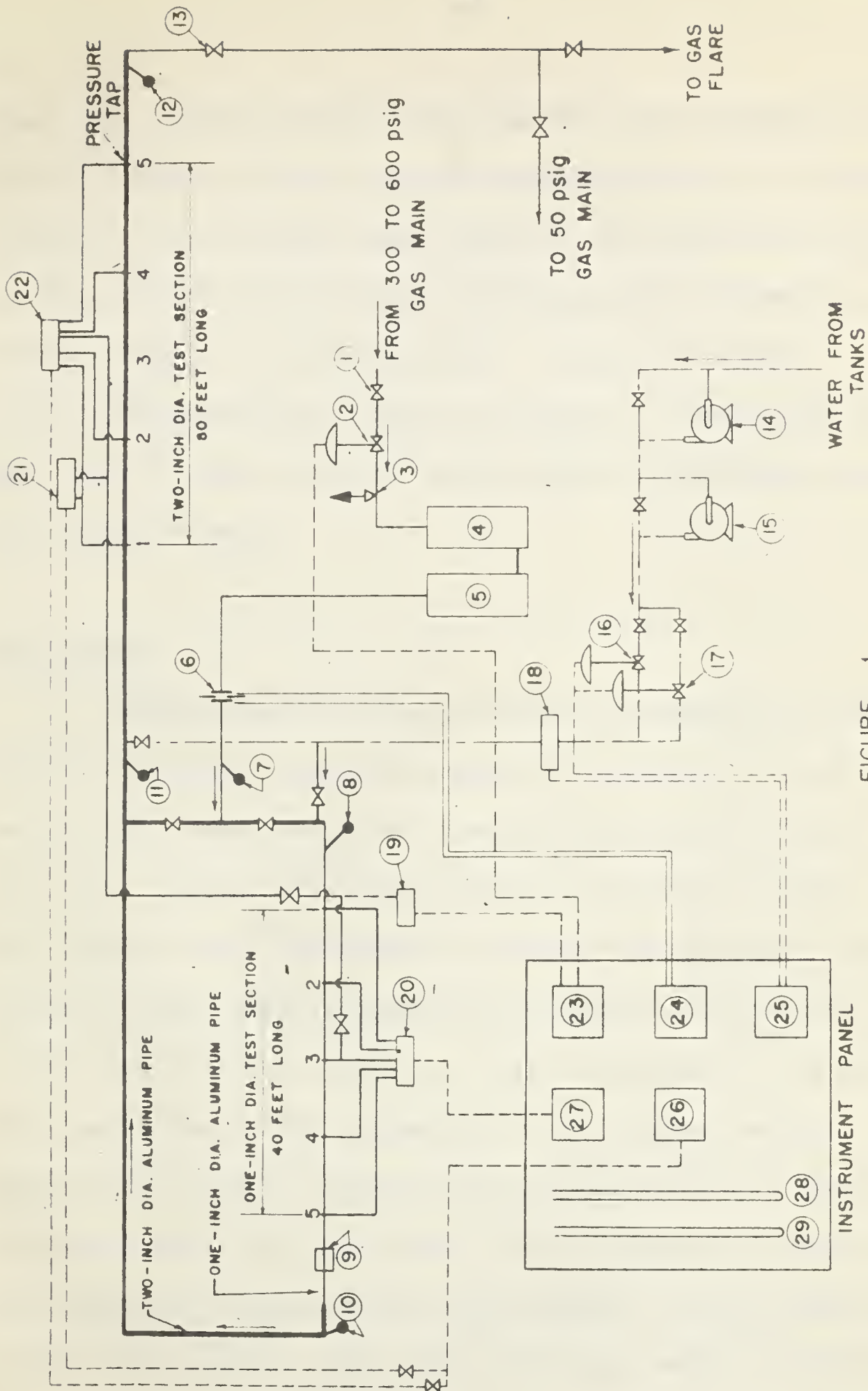


FIGURE 1

SCHEMATIC EQUIPMENT DIAGRAM

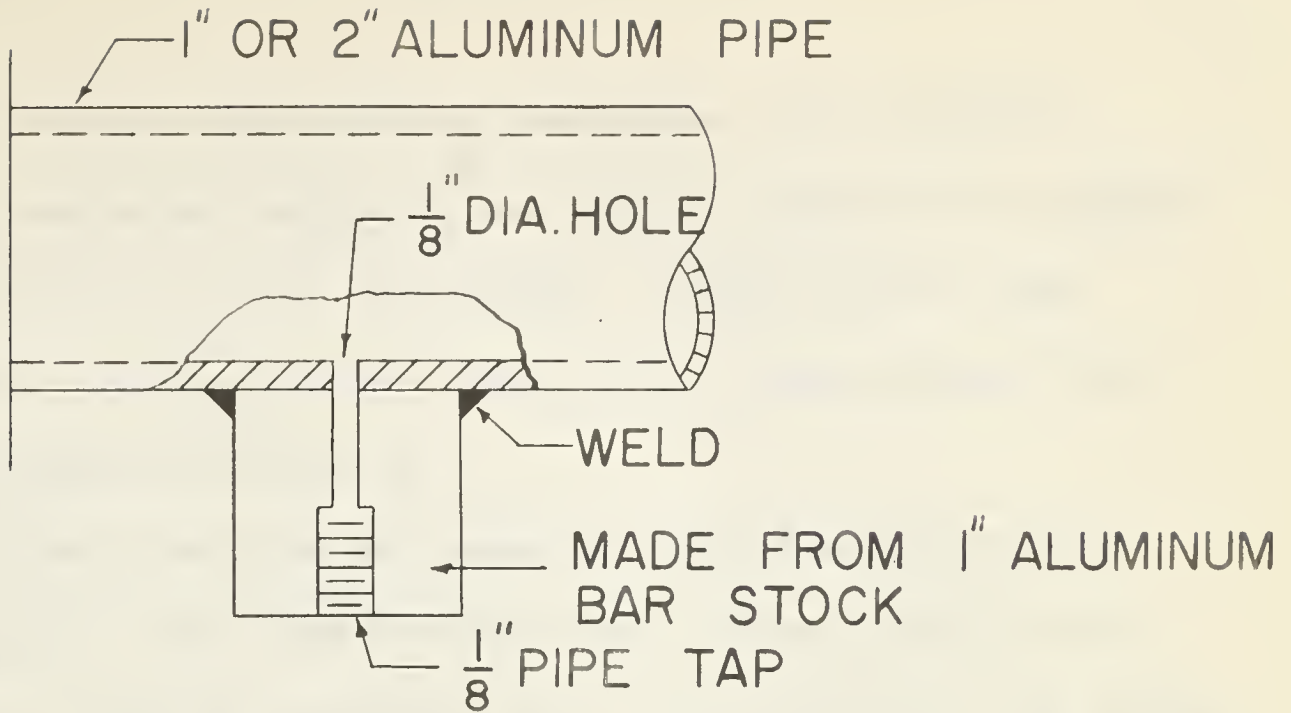
INDICATES HAND OPERATED VALVES



inch test section was 80 feet long with approximately 15 feet of the calming section upstream and downstream of the test section. Five pressure taps spaced 20 feet apart were provided on the two-inch test section. The pipe was purchased in 20-foot long sections. A welded joint is shown in Figure 2. Detail of the pressure taps is shown in Figure 3. Particular care was taken to keep the pipe smooth both at the joints and at the pressure taps.

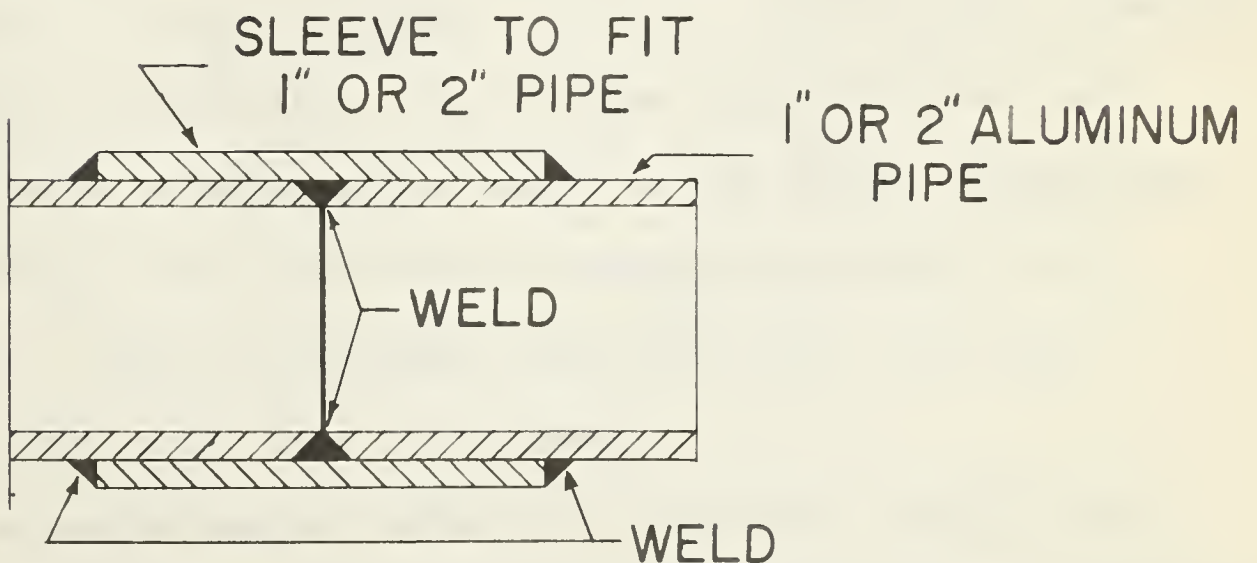
Gas System

Natural gas from the gas plant at Pembina oil field in Alberta (average composition given in Appendix A-1) was available at the City Gate Station at a variable pressure of 300 to 600 p.s.i.g. The gas was passed through a pressure control valve, two electric heat exchangers in series and an orifice flow meter to a tee where it could be directed to either the one-inch or the two-inch test section. Water was injected axially into the gas stream at the beginning of the calming section, for each section. Spray nozzles were used to spray the water into the gas stream. Gas and water from the end of the test section were taken to a flare stack approximately 300 feet from the end of the test section. The flare stack was made of a 40 foot vertical section of four-inch pipe which was located about 200



ALL INSIDE PIPE BURRS CAREFULLY REMOVED
DETAIL OF PRESSURE TAP

FIG. 3



DETAIL OF THE PIPE JOINT

FIG. 2



feet from the City Gate Station facilities. At the flare stack gas was burned and water was either evaporated or sprayed around the flare as the gas burned. During the dry gas calibration runs the gas was returned to a lower pressure gas line operating at 50 p.s.i.g.

The gas flow rate was regulated by a two-inch, single-port pneumatic valve with 3/4-inch inner valve (Fisher 667-D). The control valve was operated by a 3 to 15 p.s.i.g. air signal to the bottom of the diaphragm from a proportional plus reset controller. The input to the controller was from a pressure-transmitter installed at the mid-point of either one of the two test sections. Mid-point pressure was recorded on a chart to observe the fluctuations, if any, in the pressure. The temperature of the gas dropped to as low as 10°F during expansion through the control valve. It was then heated to above the freezing point of water and as close to the ambient temperature as possible by two electric heat exchangers (Chromolox Type GCH-6120W). The heat exchangers were of 3 K.W. and 8 K.W. capacity with on-off type controllers.

The heated gas was metered by a two-inch orifice meter constructed to American Gas Association specifications. The orifices fitting used (Senior Daniel Orifice Fitting) allowed the changing of the orifice under pressure. The static and differential

pressures were recorded on a mercury type flow recorder. The gas temperature was measured downstream of the orifice by a dial thermometer.

Water System

City water from 300-gallon water tanks was pumped by two centrifugal pumps, which could be used either individually or in series. The pumps had 3 H.P. and 5 H.P. motors respectively. The water rate was measured and controlled by an integral orifice differential pressure (D/P) cell (Foxboro Type 13 A), proportional plus reset rate controller recorder and two control valves. The control valves of 1/8-inch and 1/2-inch orifice size were installed in parallel upstream of the integral orifice D/P cell so that each valve could be used independently. Two valves were required because neither individually could give adequate control over the range of water rates desired. Two lines with independent valves were provided from the downstream of the D/P cell to the upstream of each one of the two test sections. The arrangement of the equipment is shown in Figure 1.

Pressure Drop Measurement

The pressure drop in the one-inch pipe was measured by an electrical D/P cell (Foxboro Resistance Dynalog 2400 Series) having a range of 0-600 " H₂O pressure drop and a multipoint recorder (Foxboro Dynalog). The pressure taps are numbered 1 to 5 starting at the upstream side. The manifold arrangement for the D/P cell is shown in Figure 4. At high flow rates the pressure drops between pressure points 1-2, 2-3, 3-4 and 4-5 were measured while at low flow rates the pressure drops between points 1-2, 1-3, 1-4 and 1-5 were measured. This allowed the measurement of pressure drops over the test section of up to 70 p.s.i. with a maximum estimated error of ± 6 " H₂O. The pressure drop in the two-inch pipe was measured by two pneumatic D/P cells having range of 0-100 inch H₂O pressure drop (Minneapolis Honeywell Brown Converters) and a recorder (Taylor Fulscope). The arrangement is shown in Figure 5. The pressure drops 1-3 and 3-5 were measured. At very high flow rates only the pressure drop between points 2-3 was measured.

A transparent section of lucite pipe 6" long was inserted downstream of the one-inch test section to observe and photograph the flow pattern. Plate I shows the transparent section in position.

MID-POINT PRESSURE RECORDER AND CONTROLLER

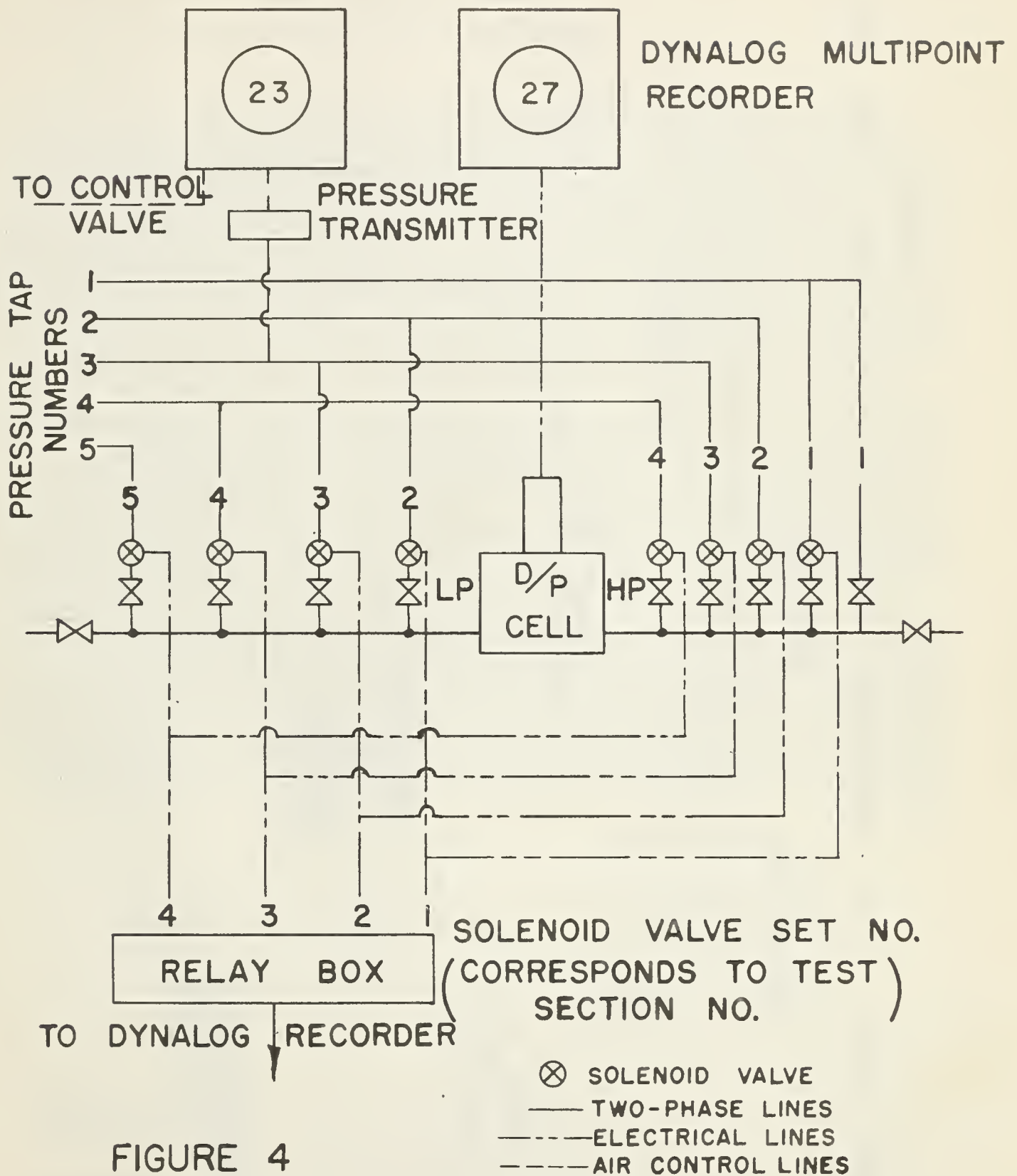


FIGURE 4

ONE-INCH PIPE PRESSURE DROP MEASUREMENT
AND MID-POINT PRESSURE CONTROL EQUIPMENT

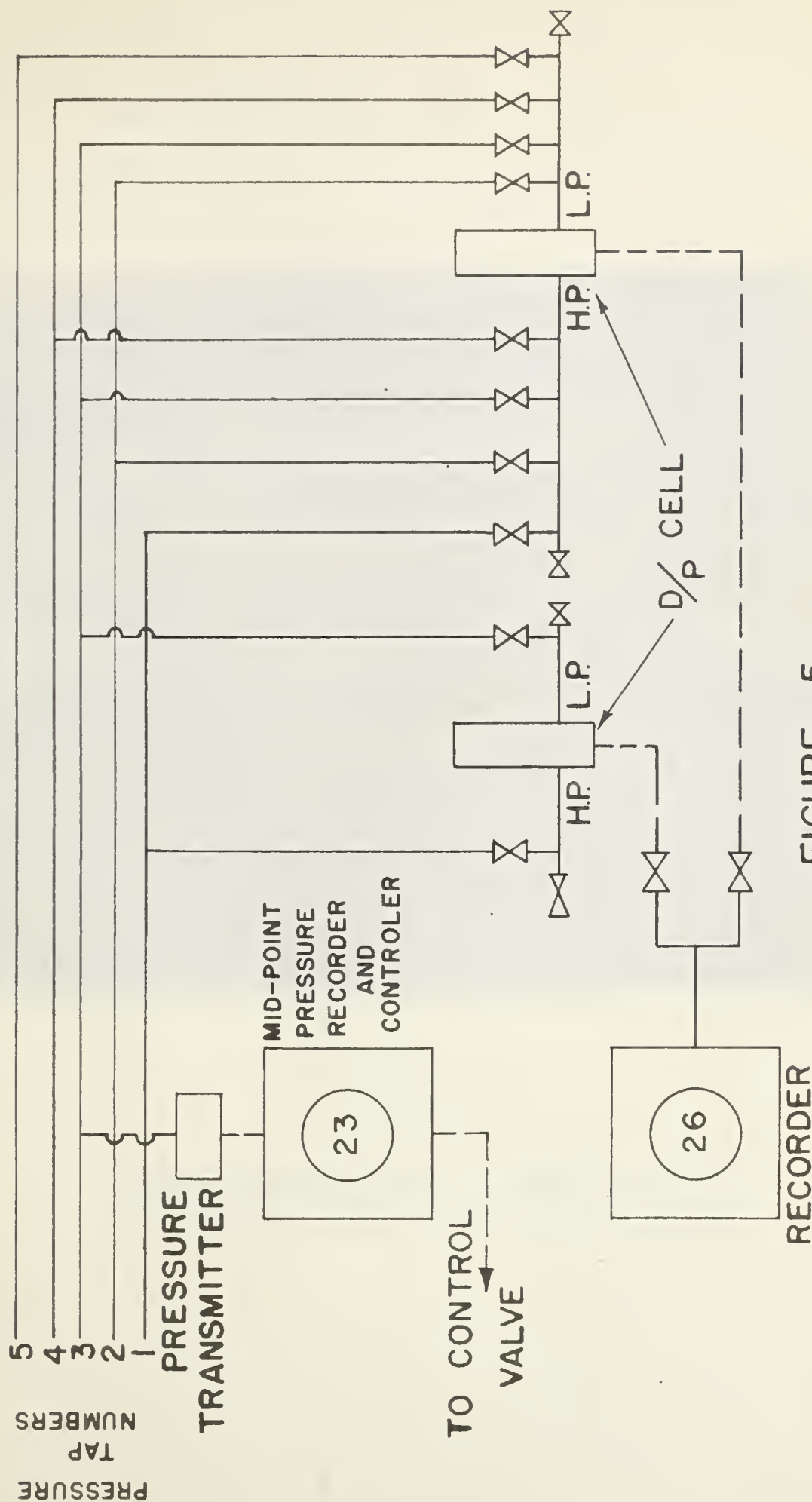


FIGURE 5

TWO-INCH PIPE PRESSURE DROP MEASUREMENT AND MID-POINT
PRESSURE CONTROL EQUIPMENT



PLATE I

TRANSPARENT SECTION IN ONE-INCH PIPE



Instrument Air Supply

For the operation of all pneumatic instruments air at a pressure of 20 p.s.i.g. was required. This air was supplied by an air-compressor through a surge tank at 100 p.s.i.g. The pressure was reduced to 40 p.s.i.g. at the outlet of the surge tank and then to 20 p.s.i.g. near the instruments. The two-stage reduction of pressure and the surge tank eliminated the pulsations caused by the reciprocating compressor. Plate II shows the compressor, air filter, surge tank and the first-stage pressure regulator.

Power Supply

Electrical power was supplied to the motors and the heat exchangers from a 3-phase, 220-volt switchboard. Overload protection switches were provided for each motor separately.



PLATE II

INSTRUMENT AIR SUPPLY

AIR COMPRESSOR AND SURGE TANK

IV EXPERIMENTAL PROCEDURE

The pressure drop and flow rate measuring equipment were first calibrated as outlined in Appendix C. The single-phase pressure drop for gas Reynolds numbers of approximately 3×10^5 to 2.5×10^6 was then obtained to determine the relative roughness of the test sections. The single-phase data are presented in Figures C-2 and C-3 of Appendix C.

Experiments were then conducted to obtain pressure drop and flow rate data for the simultaneous flow of gas and water at a constant mid-point pressure and temperature. A mid-point pressure of 120 p.s.i.g. was selected. Actually, it was only possible to maintain the mid-point pressure between 118 and 121 p.s.i.g. and the average temperature between 36°F and 73°F. Most of the data, however, was obtained at a constant mid-point pressure of 120 p.s.i.g. and an average temperature of about 50°F. The superficial water velocities were varied for the one-inch pipe from 0.0067 ft./sec. to 2.42 ft./sec. and for the two-inch pipe from 0.00303 ft./sec. to 0.525 ft./sec. The superficial gas velocities were varied for the one-inch pipe from 40 ft./sec. to 300 ft./sec. and for the two-inch pipe

from 25 ft./sec. to 130 ft./sec. The pressure drop data were obtained at constant superficial water velocities by varying the superficial gas velocities over the range. Water required to saturate the gas for any gas velocity was calculated and added to the water required to maintain a certain constant superficial water velocity in the pipe line. This water rate was then set on the water flow controller. For high water rates the amount of water required to saturate the gas was negligible. The variables measured are presented in Table 1.

TABLE 1

DATA OBTAINED

GAS FLOW MEASUREMENT (2" Orifice Meter)

Orifice size in inches

Static pressure (Downstream) in p.s.i.g.

Differential pressure in inches of water

Gas temperature in °F

Atmospheric pressure in p.s.i.a.

WATER FLOW MEASUREMENT (Integral Orifice D/P cell)

Orifice size in inches

Differential pressure in inches of water

ONE-INCH TEST PIPE (1.049-inch internal diameter)Pressure drops between pressure taps 1-2, 2-3,
3-4 and 4-5 in inches of water

Mid-point pressure (at pressure tap 3) in p.s.i.g.

Upstream temperature in °F

Downstream temperature in °F

TWO-INCH TEST PIPE (1.067-inch internal diameter)Pressure drop between pressure taps 1-3 and 3-5 in
inches of water

Two-Inch Test Pipe (Continued)

Mid-point pressure (at pressure tap 3) in p.s.i.g.

Upstream temperature in °F

Downstream temperature in °F

WATER CONTENT OF THE GAS

Weight of the desiccant tube before gas flow in grams

Gas flow through the desiccant in cubic feet at the
temperature of gas and 2 to 6 inches of water
above atmospheric pressure

Weight of the desiccant tube after the measured gas
flow through the desiccant in grams

Experimental data at approximately constant superficial gas velocity, constant superficial water velocity and variable mid-point pressure was obtained by establishing critical flow conditions at the downstream back pressure control valve. When the pressure upstream of the valve was about two times or more the pressure downstream of the valve, the superficial gas velocity was constant.

V EXPERIMENTAL RESULTS

The composition and properties of the gas and the geometry of the system are presented in Tables A-1 and A-2 of Appendix A. Appendix B contains all of the pressure drop data. Section B-9 of Appendix B describes the calculation procedure for the calculated data in this Appendix. The calibration data and other information regarding the calibration of the equipment are included in Appendix C.

Single-phase

The results of the tests with gas flowing alone are given in Appendix B in Tables B-1 and B-3 for the one-inch pipe and Tables B-2 and B-4 for the two-inch pipe. The integrated form of the Fanning equation (16) for gas flow was used to calculate the friction factor for each of the four 10-foot long sections of the one-inch test pipe. Since for certain of the tests the Reynolds numbers were sufficiently

$$Q = 1.61 \frac{T_o}{P_o} \left[\frac{(P_1^2 - P_2^2) d^5}{G T L f Z_a} \right]^{0.5} \quad (16)$$

where Q = gas flow measured at T_o and P_o , std. cu.
ft. per hr.

L = length of line, miles

d = internal diameter (I.D.), in.

P_1 = upstream pressure

P_2 = downstream pressure

G = gas gravity (air = 1.0)

Z_a = average compressibility factor

f = Fanning friction factor

high that fully developed turbulence was to be expected. The friction factor for these tests was assumed independent of Reynolds number and is a function only of the relative roughness. The equation of Nikuradse was then used to calculate the relative roughness for each section. The single-phase data are presented for each of the sections of the one-inch pipe in Figure C-2 of Appendix C. The average relative roughnesses for the various sections of the one-inch pipe were 0.00006, 0.00009, 0.00015 and 0.0002.

An average value for the mid-point relative roughness was then obtained by calculating the slope of the pressure versus length curves at this point for all of the flow rates.

This slope was then used to calculate the friction factors by the differential form of the Fanning equation. A similar procedure was followed for the two-inch pipe. The friction factor versus Reynolds number curves for the two pipes are presented in Figure C-3 of Appendix C. The data for the one-inch pipe are best represented by the Colebrook equation for $\frac{e}{D} = 0.00009$ and the data for the two-inch pipe by the equation for $\frac{e}{D} = 0.000048$. The Colebrook curves for these two relative roughnesses are also shown on Figure C-3. The relative roughness for the two-inch pipe is approximately one half that of the one-inch pipe. This gives approximately the same absolute roughness of 0.00009 inches for the two sizes of aluminum pipe. This is a reasonable value for the roughness of aluminum pipe, confirming the technique. A good check was also obtained between the calculated and the experimental data for single-phase flow as shown in Figures 7 and 8.

Two-phase Data

The experimental and calculated two-phase data are tabulated in Appendix B. Tables B-1 and B-2 contain the experimental data for the one- and two-inch pipes respectively,

while tables B-3 and B-4 contain the calculated data. The calculated data in these tables consist of the gas-phase density at the mid-point, the superficial velocities of the two phases, the mid-point pressure gradient and the mid-point pressure gradient adjusted to a constant gas density of 0.47 lbs. per ft.³

The two-phase pressure gradient at the mid-point of the test section, $(\frac{dP}{dL})$, was also obtained by measuring the slope of the pressure versus length curves at this point for each test. Typical pressure gradient curves for the one-inch pipe are shown in Figure 6 for various flow rates.

Figures 7 and 8 and Tables B-3 and B-4 represent the basic pressure drop data adjusted to a constant gas density for the two pipes. The figures show the pressure gradient plotted against the superficial gas velocity for various constant superficial water velocities. The single-phase calculated lines and experimental data points are also shown in Figures 7 and 8 for comparative purposes. The single-phase lines were calculated by assuming relative roughnesses of 0.00009 and 0.000048 for the one- and two-inch pipes respectively.

Cross plots of the data of Figures 7 and 8 are presented in Figures 9 and 10 respectively. These show the pressure

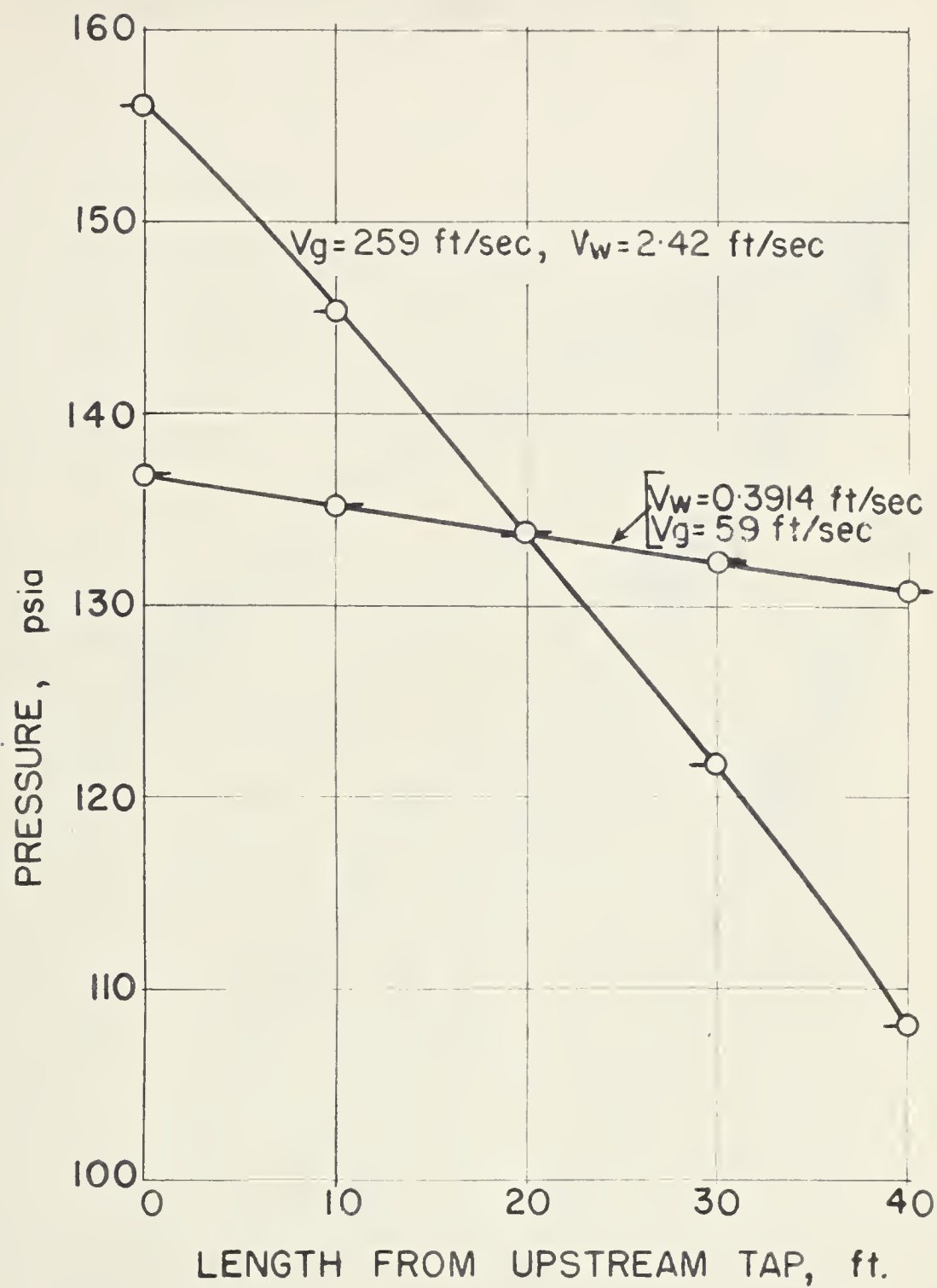
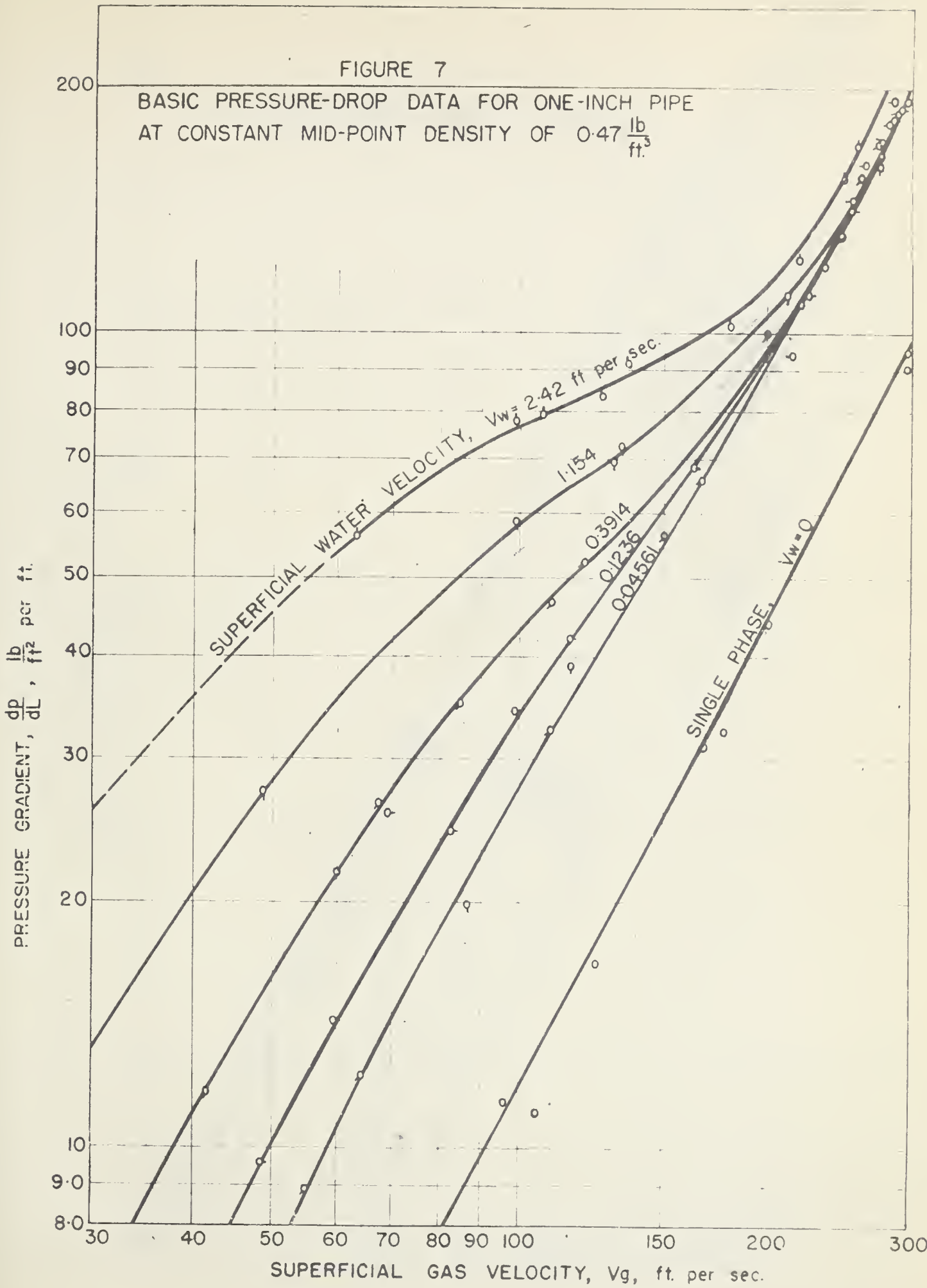
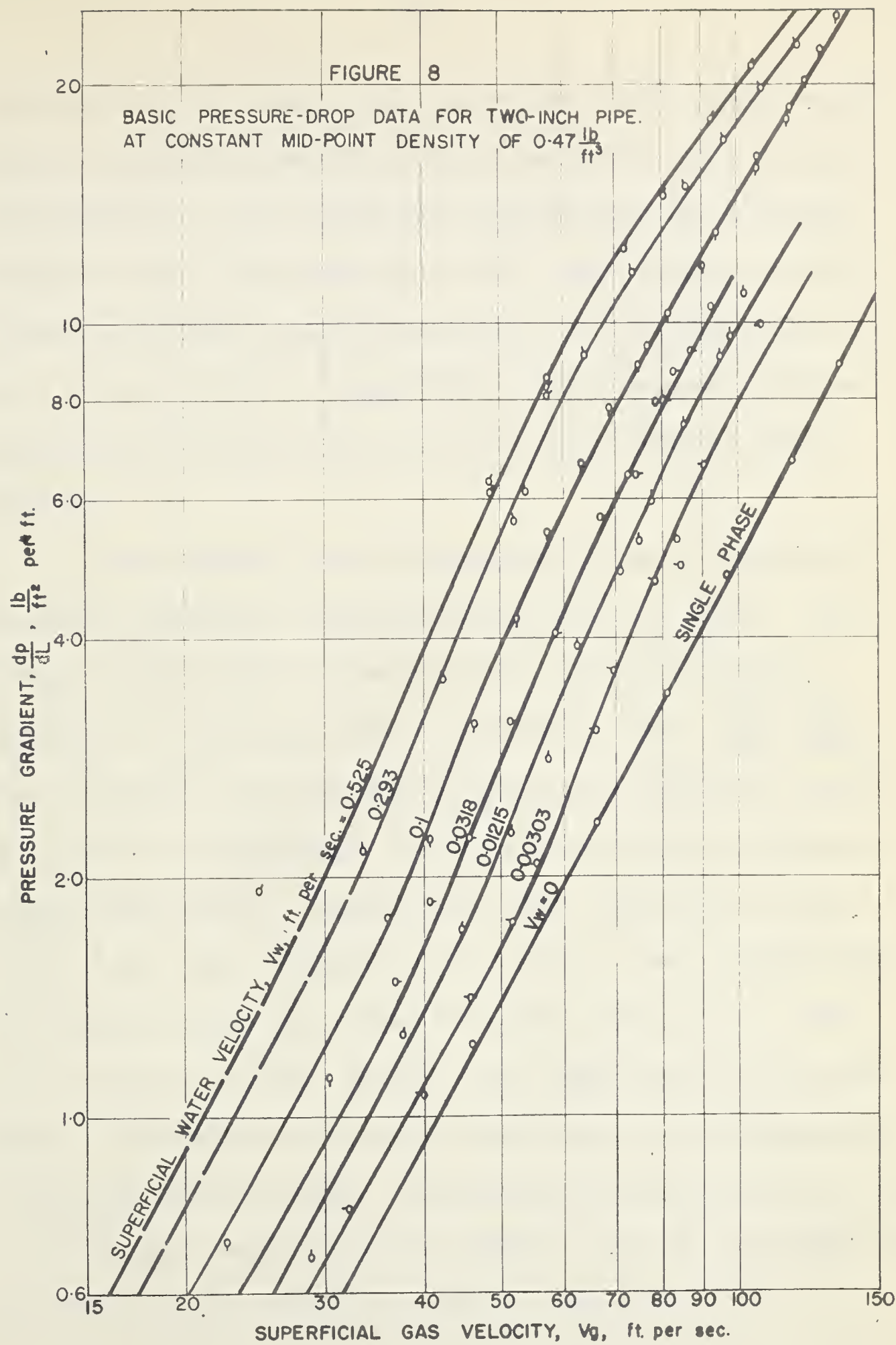


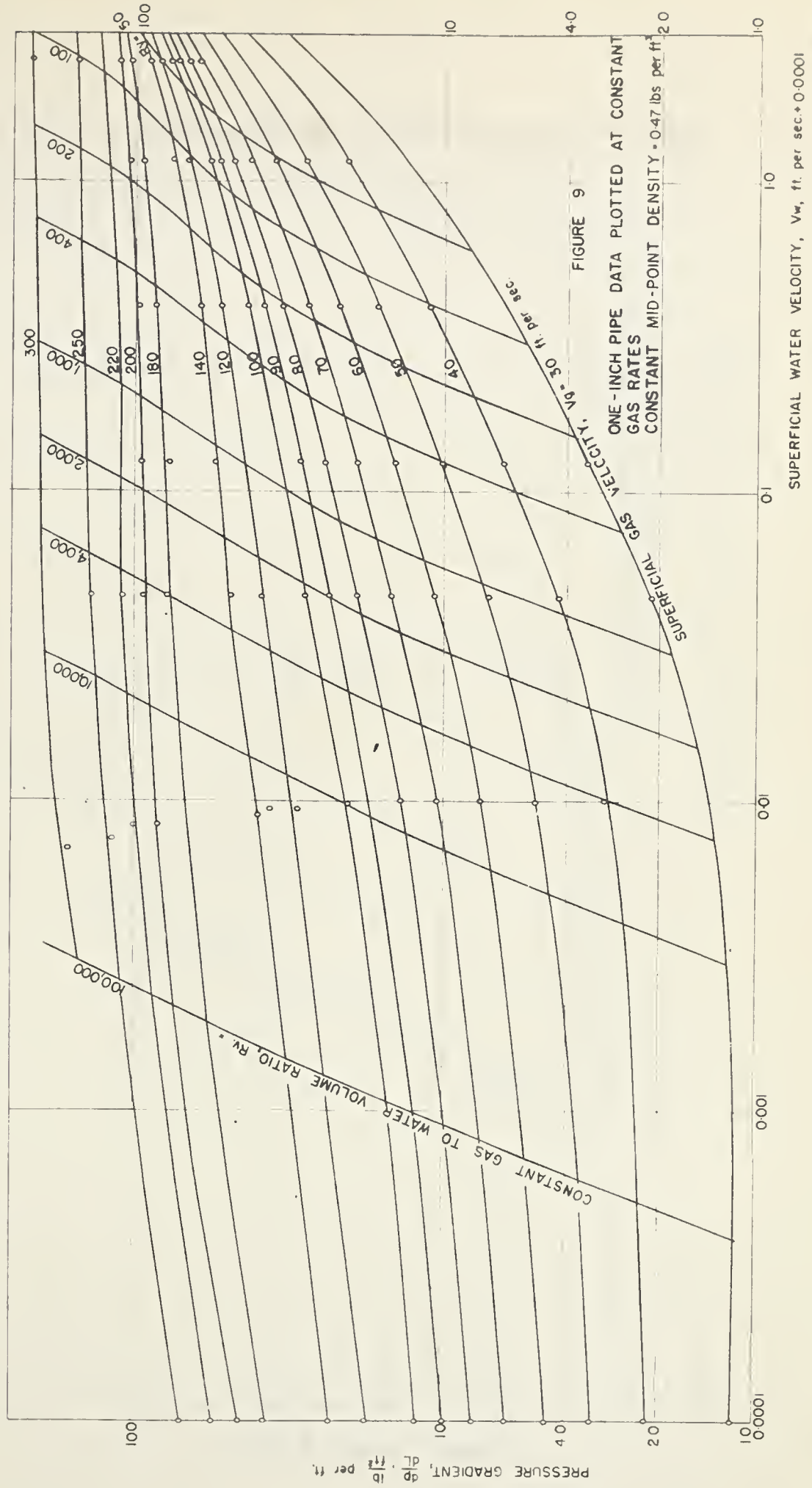
FIGURE 6
TYPICAL ONE-INCH PRESSURE GRADIENT.

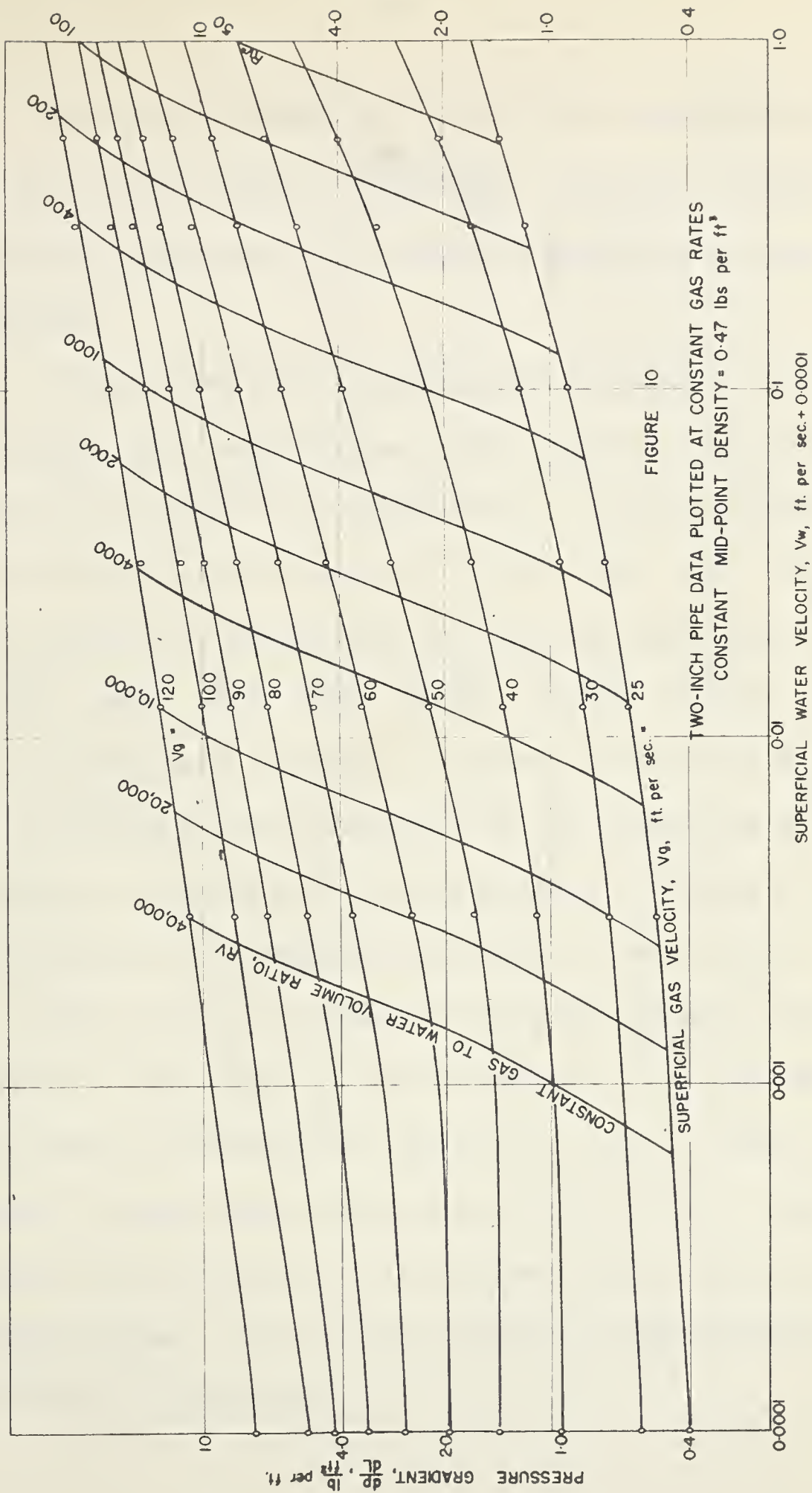




gradient plotted against the superficial water velocity for various constant superficial gas velocities. The data are extrapolated to the appropriate single-phase gas pressure gradient values (the addition of the small constant to the superficial water velocity permitted the representation of zero water velocity on logarithmic coordinates). Lines of constant gas-liquid volume ratio are also shown on these figures.

From Figures 9 and 10, smoothed pressure drop data at selected superficial water velocities were obtained. From these smoothed data the ratio of the two-phase pressure gradient to the single-phase pressure gradient, $(\frac{dP}{dL}) / (\frac{dP}{dL})_g$, was calculated. The calculated data are tabulated in Table B-5 and B-6 of Appendix B for the one- and two-inch diameter pipes respectively. Superficial water velocities of 0.01, 0.03, 0.10, 0.30, 1.0 and 3.0 ft. per sec. were selected for the one-inch pipe and values of 0.001, 0.003, 0.010, 0.03, 0.10, 0.30 and 1.0 ft. per sec. were taken for the two-inch pipe. The highest velocity in each case is an extrapolation of the experimental data. Superficial gas velocities for the one-inch pipe ranged from 30 to 300 ft. per sec. and those for the two-inch pipe from 25 to 120 ft. per sec.

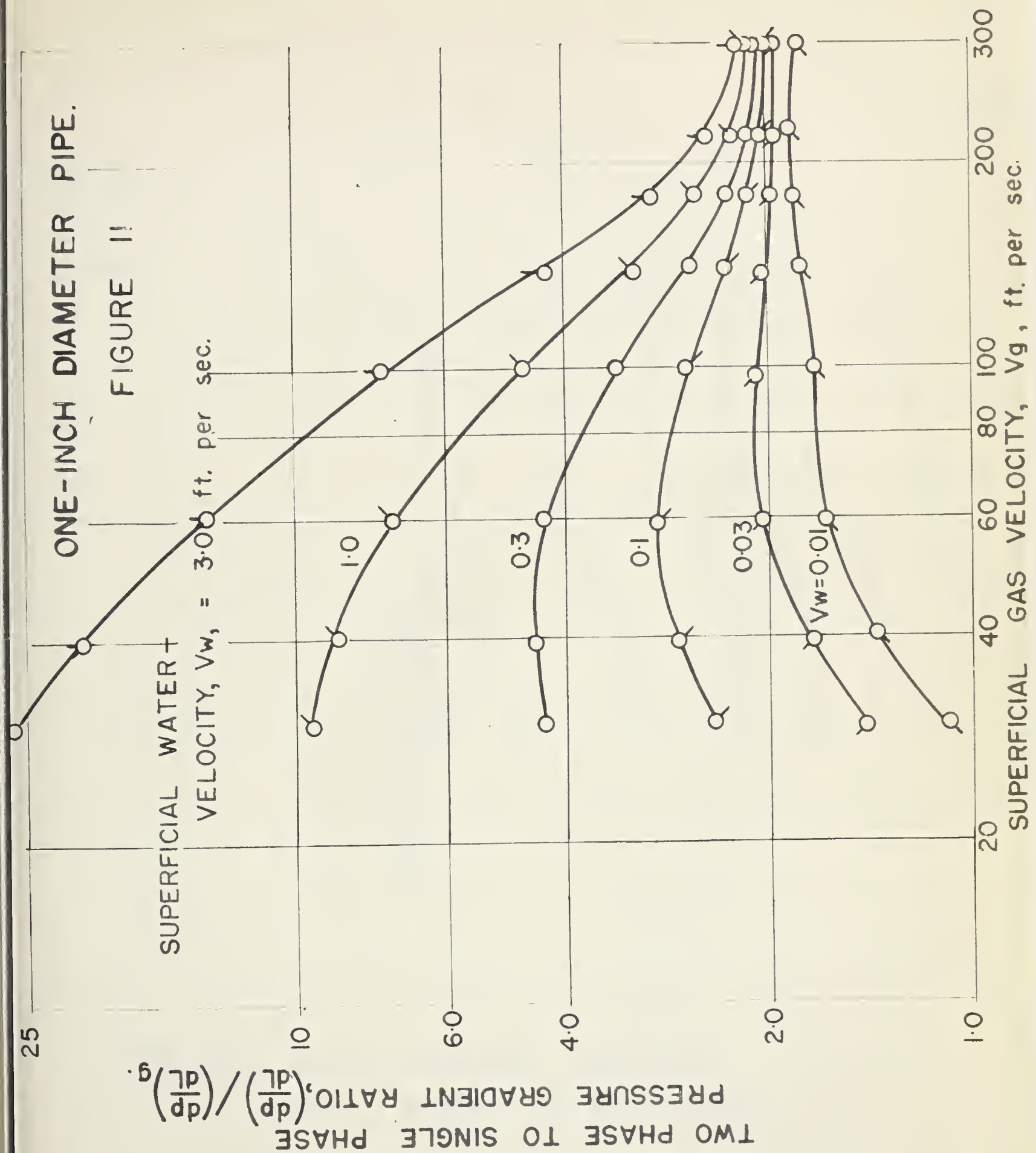




The data of Tables B-5 and B-6 are represented by Figures 11 and 12 where $(\frac{dP}{dL})/(\frac{dP}{dL})_g$ is plotted against the superficial gas velocity for various superficial water velocities.

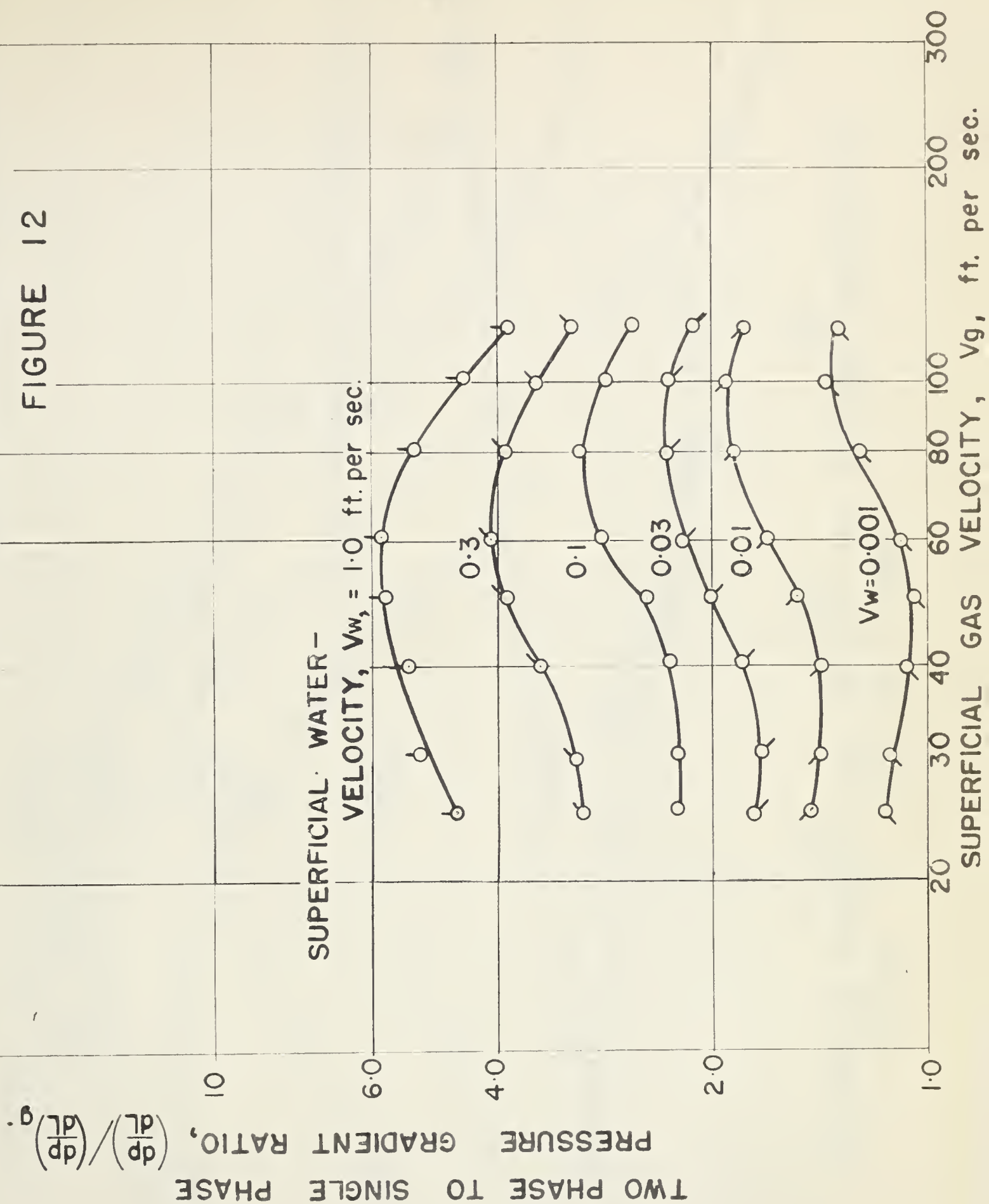
The data were also obtained from Figures 9 and 10 at constant gas-liquid volume ratios and are tabulated in Tables B-7 and B-8 of the Appendix B. For the one-inch pipe, gas to liquid volume ratios of 50, 100, 200, 400, 1000, 2000, 4000, 10,000, and 100,000 and for the two-inch pipe 40, 100, 200, 400, 1000, 2000, 4000, 10,000, 20,000, 40,000, 100,000 and 1,000,000 were selected. Figures 13 and 14 represent the data of Tables B-7 and B-8 where the friction factor based on mixture properties is plotted against the Reynolds number of the mixture for constant gas-liquid volume ratios.

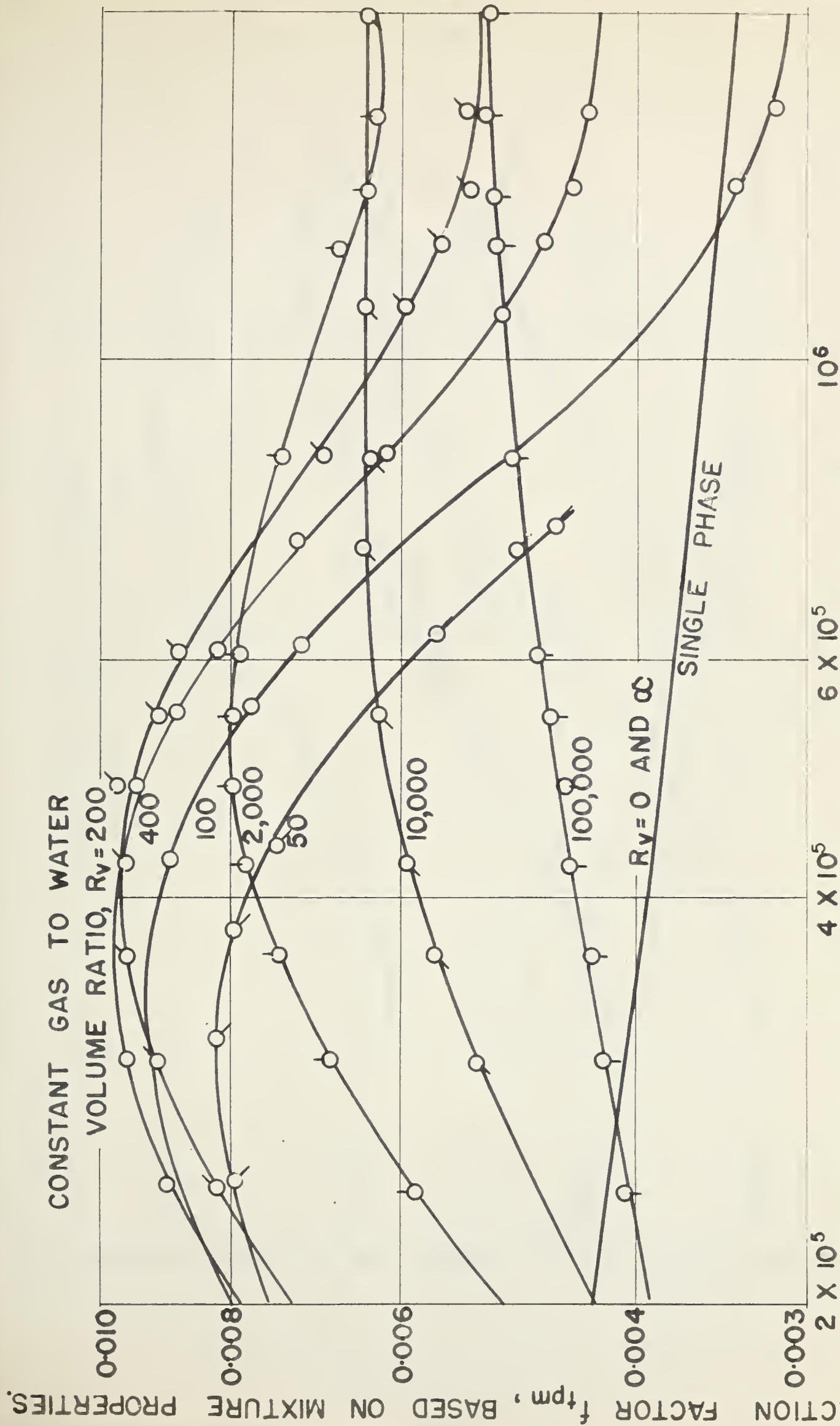
Limited data at variable mid-point density and constant superficial velocities of the two-phases were also obtained. These data are included in Tables B-1, B-2, B-3 and B-4 of Appendix B along with the constant density data. Figure 15 indicates the variation of the pressure drop ratio (two-phase to single-phase) with the gas density at approximately constant flow rates of the phases.



TWO-INCH DIAMETER PIPE.

FIGURE 12





REYNOLDS NUMBER Re_m , BASED ON MIXTURE PROPERTIES.
FIGURE 13, ONE-INCH PIPE.

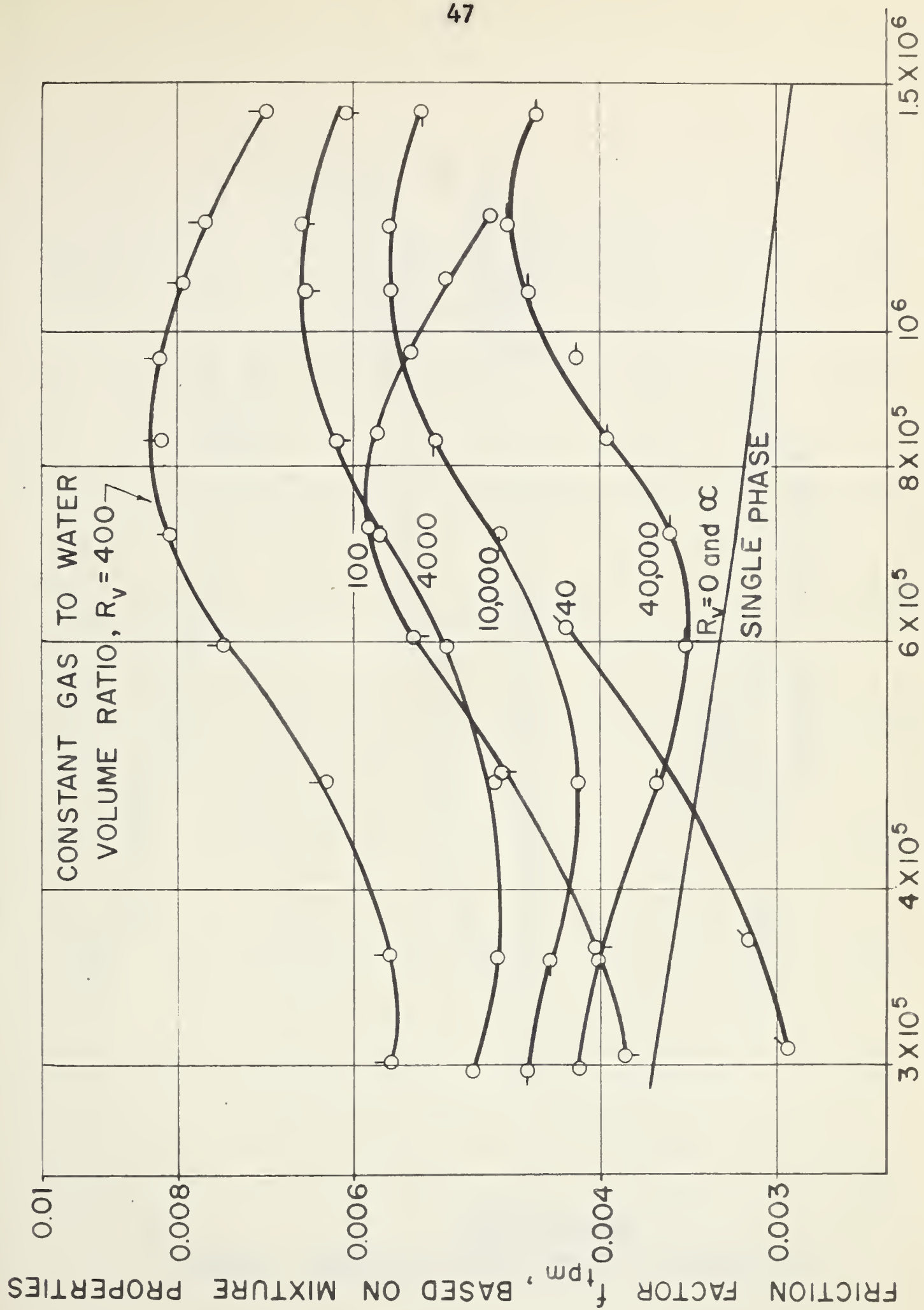
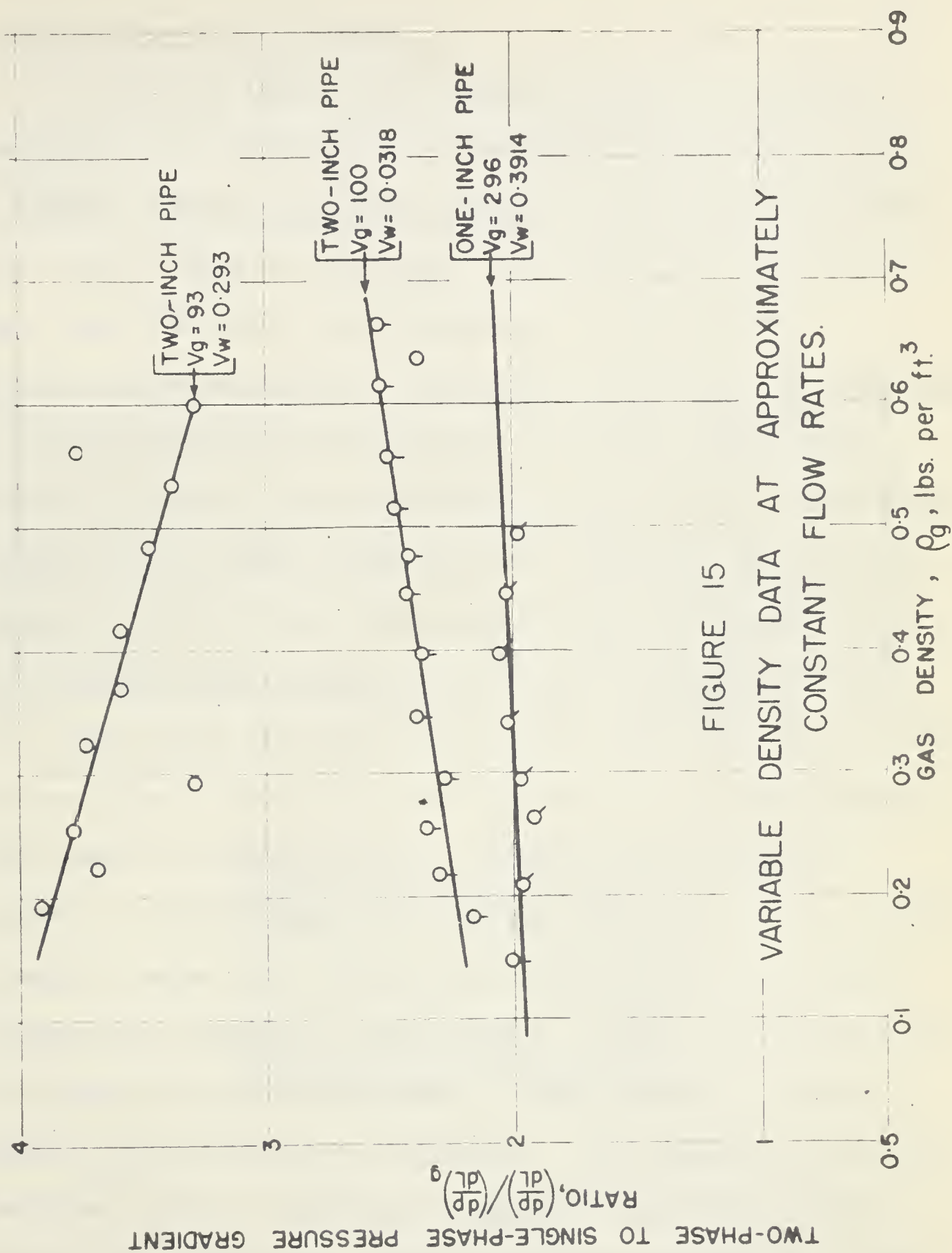


FIGURE 14, TWO-INCH PIPE



Observation of Flow Pattern

The flow pattern was observed through a transparent section of one-inch pipe over the range of flow rates investigated. Visual observations showed a milky colour mist over the entire range of flow rates. At high water rates and low gas rates there was some indication of surface waves on the inside pipe wall. Considerable difficulty was experienced in photographing the flow pattern. A 35 mm. camera with shutter speeds as fast as $1/1000$ sec. and a movie camera with speeds of up to 8000 frames per sec. (effective exposure per frame of $1/24,000$ sec.) were used. Three photographs of the flow pattern are included in Plate III. Photograph 1 taken at a high water rate and low gas rate shows the surface waves in the liquid film on the inside pipe wall. At approximately the same gas velocity and a low liquid rate Photograph 2 shows no surface waves. At high gas rates and over the entire range of water rates photographic observations of the flow pattern were similar to Photograph 3. There is no indication of surface waves in Photograph 3. This, however, does not mean a liquid film was not present. The location of the test equipment made it difficult to properly light the flow for photographic purposes. Better photographic techniques might show the liquid film that probably is present at these velocities.



Photograph 1 $V_g = 60$ ft./sec., $V_w = 2.42$ ft./sec.



Photograph 2 $V_g = 60$ ft./sec., $V_w = 0.4$ ft./sec.



Photograph 3 $V_g = 300$ ft./sec., $V_w = 0.4$ ft./sec.

VI DISCUSSION OF RESULTS

The experiments have indicated a large effect of a small quantity of water on the pressure drop in the pipeline flow of gas at high velocities. This effect may best be shown by plotting the ratio of the two-phase pressure gradient to the single-phase pressure gradient as a function of the superficial gas velocity. In this type of representation either gas-liquid volume ratio or the liquid rate may be the parameter. Figures 11 and 12 are representations of this type for the one- and two-inch diameter pipes with the water rate as the parameter. The diameter and the roughness of the pipe have different effects on the flow pattern, and hence on the pressure drop, at different flow rates. The pressure gradient ratio for high water rates drops sharply as the gas rate is increased. This same effect, however, is not observed for the two-inch pipe. At a superficial gas velocity of 30 ft. per sec. and a superficial water velocity of 1.0 ft. per sec., the pressure gradient ratio, $\frac{dP}{dL} / (\frac{dP}{dL})_g$, for the one-inch diameter pipe is 9.5 and for the two-inch pipe, 4.8. At a higher superficial gas velocity of 100 ft. per sec.

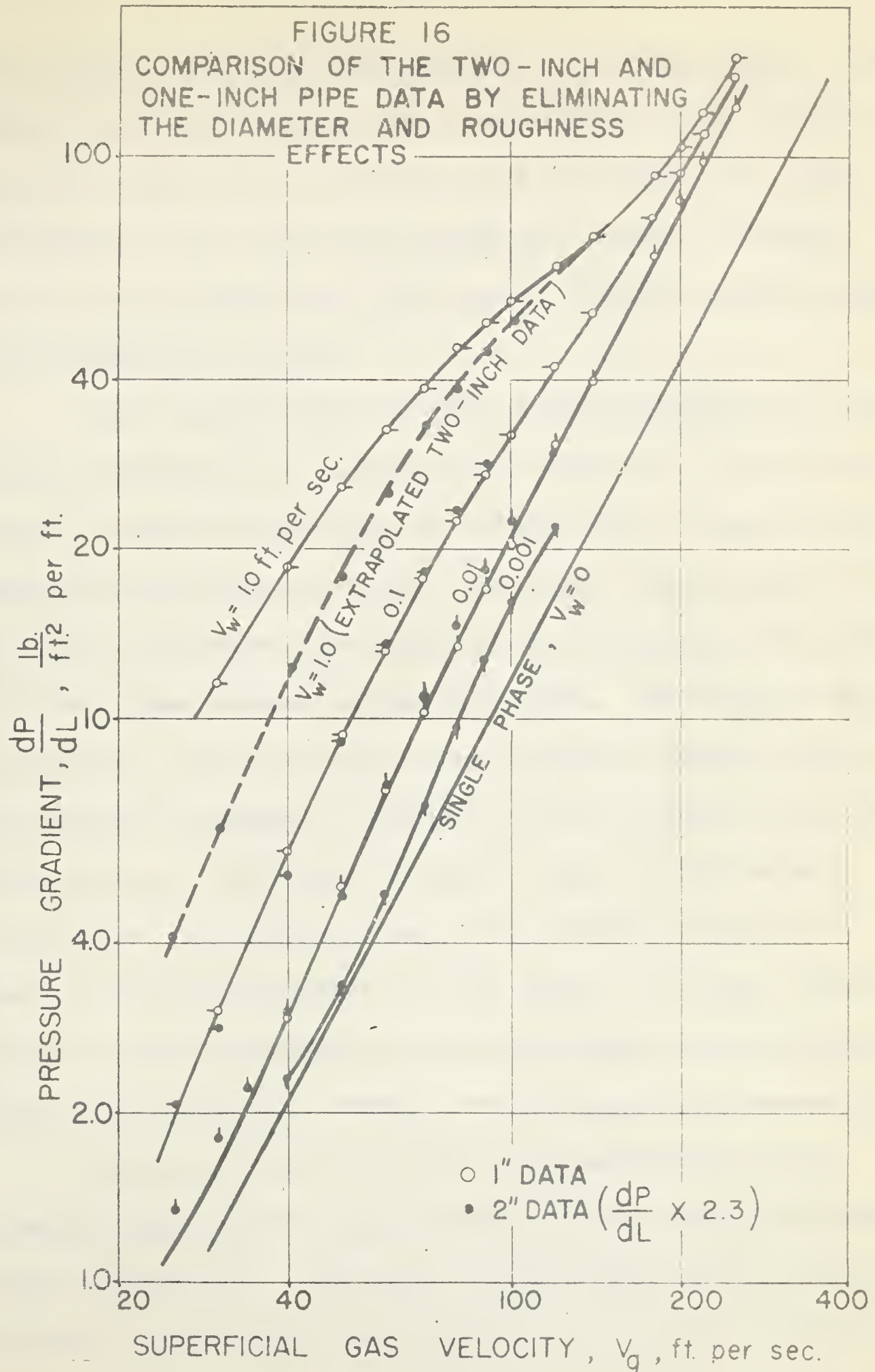
and the same water rate the pressure gradient ratio for the one-inch pipe drops to 4.7 and for the two-inch pipe to 4.5.

The pressure gradient ratio curves for the two-inch diameter pipe exhibit maximum and minimum values and behave similarly over the range of flow rates investigated. At lower water flow rates the effect of diameter on the flow pattern seems to be small and the pressure gradient ratio curves for the one-inch pipe are similar in shape to the curves for the two-inch pipe. Below a superficial gas velocity of approximately 200 ft. per sec. the pressure gradient ratio in the one-inch diameter pipe decreases with increasing gas rate. Further increase in gas velocity to 300 ft. per sec. causes little change in the pressure gradient ratio, especially for low water rates. The maximum superficial gas velocity investigated in the two-inch diameter pipe was 120 ft. per sec. Figure 12 for the two-inch pipe shows a fairly sharp drop in the pressure gradient ratio for high water rates as the gas velocity is increased from about 60 to 120 ft. per sec. The data indicate that at higher velocities the effect of water rate on pressure drop decreases in the two-inch diameter pipe in a manner similar to the one-inch diameter pipe.

Although all of the data are in the annular-mist flow region, the changes in shape of the curves may be interpreted

as representing the microscopic changes in flow pattern. This is particularly clear from the two-inch data as shown in Figure 12. The loci of the maxima and the minima of these curves divide the data into three regions. The changes in film thickness and the film surface characteristics are probably the more important factors influencing the shape of these curves.

The single-phase pressure drop lines, as shown by Figures 7 and 9 are almost straight and parallel for the two test pipes over the range of gas velocities investigated. The difference in the diameter and roughness effect between the two pipes may be eliminated for single-phase flow by multiplying the two-inch pipe pressure gradient by 2.30. The factor 2.30 is the ratio of the pressure gradients for the two pipes in single-phase gas flow. Figure 16 shows the actual pressure gradient for the one-inch pipe and the pressure gradient multiplied by 2.30 for the two-inch pipe at superficial water velocities of 0, 0.01, 0.1 and 1.0 ft. per sec. for both pipes. The agreement between the data of two pipe sizes is good for water velocities of 0.01 and 0.1 ft. per sec. The superimposition of the curves at low water rates shows the small effect of diameter on flow pattern. At a higher water velocity of 1.0 ft. per sec. the effect of diameter increases



and the data cannot be superimposed in the same manner. The data for the two-inch pipe at a superficial water velocity of 1.0 ft. per sec. are extrapolated from Figure 10. This correlation may be used for estimating two-phase pressure drops in the annular-mist flow region in small diameter pipes at low water flow rates.

For a generalized solution of the two-phase flow problem it is advantageous to represent the behaviour of both of the phases in single-phase flow by a single line. Lines on the same plot for various constant gas-liquid volume ratios can then be used to represent the two-phase flow behaviour. The shape of these lines depends on the flow rates. This may be done by defining a friction factor and a Reynolds number based on the mixture properties. Teletov (15) has defined a friction factor, f_{tpm} , and a Reynolds number, Re_m , in this manner. There is no real physical basis for defining the friction factor and Reynolds number in this manner. It does, however, allow the representation of the single-phase gas and single-phase liquid flow by a single line on f_{tpm} , Re_m coordinates.

Figures 13 and 14 are such representations of the pressure drop data for the one-inch and the two-inch diameter pipes respectively. This type of plot shows how the deviation from the single-phase line increases as the liquid rate is

increased, goes through a maximum and then decreases. The deviation from the single-phase line is a function of the Reynolds number, the gas-liquid volume ratio and the pipe diameter for the fluids investigated.

Teletov (15) has shown this deviation to be a function of the gas-liquid volume ratio and the fluid viscosity ratio only. Insufficient data are presented by Teletov to allow a critical evaluation of his work.

Over the range of gas rates investigated the single-phase friction factor is fairly constant, especially for the one-inch pipe. This makes the single-phase pressure drop directly proportional to the gas density. The limited two-phase data taken at variable density clearly indicates that the two-phase pressure drop is not directly proportional to the gas density or the mixture density at approximately constant superficial liquid and gas velocities. It is shown by Figure 15 that the effect of density is influenced by the liquid and the gas rates, and the pipe size. In the annular-mist flow region the two-phase pressure drop is not a single valued function of the superficial Reynolds number only. This makes difficult the interpretation of the data of other investigators who have not maintained a constant mid-point density.

The experimental work for this investigation was conducted at carefully controlled, constant mid-point pressure.

The manner in which the two phases orient themselves in the pipe has a great effect on the energy loss due to irreversibilities. The higher viscosity fluid, liquid in this case, when travelling in an annular film against the pipe wall, will cause a greater loss of energy than if the same amount of liquid were travelling in the same gas stream as a dispersed phase. The proportion of liquid in the dispersed phase increases as the gas velocity is increased. This explains the greater displacement from the single-phase pressure drop of the two-phase line for high water rates at low gas rates. The effect of gas velocity on the film thickness seems to be more pronounced in the one-inch pipe than in the two-inch pipe. Other factors which would be expected to influence the pressure drop are the shape of the liquid film, distribution of the liquid droplets in the gas phase, the impingement of the liquid droplets on the liquid surface and formation and collapse of the surface waves.

The comparison of these data with those of other investigators and the testing of various correlations was considered. There are no data available in the literature for

the range of variables investigated in this work, making any direct comparison impossible. Considerably more work is required to resolve the effect of the physical properties of the flowing stream and make possible a comparison with data obtained for different systems. The correlation of Lockhart and Martinelli (7) has been considered by other investigators (7, 8) and has been found not suitable in this region.

The analyses of Calvert and Williams (17) and others (14, 15, 16, 18 and 19) could be applied to these data to separate the water flow rates in the film and the gas core. These flow rates could then be considered separately to calculate the energy loss due to irreversibilities. This work, however, is planned as a separate study.

Further investigations are required, and are underway at the University of Alberta, to resolve the effect of gas density, liquid and gas properties and flow rates and pipe size.

VII CONCLUSIONS

1. A mechanistic approach is necessary for a better understanding of the two-phase flow phenomenon.
2. The pressure drop may be greatly affected by microscopic changes in the flow pattern within the general annular-mist region.
3. Liquid in the annular film causes greater energy loss than the same liquid in the gas core.
4. Very small addition of water to a high velocity gas stream causes a large increase in pressure drop by forming a liquid film on the inside pipe wall.
5. At higher water rates the proportion of the water in the film is higher for lower gas velocities.
6. All investigations should be conducted wherever possible at constant mid-point conditions.

NOMENCLATURE *

A	=	cross-sectional area of the pipe,	sq. ft.
D	=	inside diameter of pipe,	ft.
f	=	friction factor,	dimensionless
g_c	=	dimensional conversion constant,	$\frac{\text{lb. (mass)}}{\text{lb. (force)}} \frac{\text{ft.}}{\text{sec}^2}$
L	=	length of the test section,	ft.
P	=	pressure,	lbs. per sq. in.
R_e	=	Reynolds number,	dimensionless
T	=	temperature of fluid at average conditions,	$^{\circ}\text{R}$
$\frac{\Delta P}{\Delta L}$	=	pressure drop per unit length,	$\frac{\text{lbs.}}{\text{ft.}^2}$ per ft.
$\frac{dP}{dL}$	=	pressure gradient at the mid-point	$\frac{\text{lb.}}{\text{ft.}^2}$ per ft.
$\frac{(\frac{dP}{dL})}{(\frac{dP}{dL})_g}$	=	ratio of the two-phase pressure gradient to the single-phase pressure gradient if the same quantity of gas was flowing alone in the pipe at the same mid-point conditions,	dimensionless
R_m	=	input gas-liquid massratio,	dimensionless
R_v	=	input gas-liquid volume ratio at mid-point conditions,	dimensionless

* Special terms have been defined in their proper context.

- v = specific volume of the liquid at mid-point flow conditions, cu. ft. per lb.
- V = superficial velocity of fluid at mid-point conditions based on total pipe cross-section, ft. per sec.
- ρ = density of fluid at mid-point conditions lbs. per cu. ft.
- μ = absolute viscosity of the fluid at average mid-point conditions lbs. per ft. sec.

Subscripts

- g - refers to the gas phase or values calculated using the gas-phase properties
- l - refers to the liquid phase in general or values calculated using the liquid-phase properties
- w - refers to the water or values calculated using the water properties
- tp - refers to the two-phase flow
- tpg - refers to two-phase flow but calculated using gas properties
- tpm - refers to two-phase flow but calculated using mixture properties
- 1,2,3,4,5 - refer to the pressure taps on each test section starting at the upstream end

BIBLIOGRAPHY

1. Omer, M.M., "The Horizontal Pipeline Flow of Air-Water Mixtures", M.Sc. Thesis, University of Alberta, April, 1960.
2. Wood, R.K., "The Upward Vertical Flow of Oil-Water Mixtures", M.Sc. Thesis, University of Alberta, March, 1960.
3. Bennett, J.A.R., "Two-phase Flow in Gas-Liquid Systems - A Literature Survey", U.K. Atomic Energy Authority, AERE CE/R 2497, 1958.
4. Nikuradse, J., VDI - Forschungsheft 361, 1933.
5. Karman, T. von., NACA TM 611, 1931.
6. Colebrook, C.F., J. Inst. Civil Engrs. (London), 11, 133, 1938-1939.
7. Lockhart, R.W. and Martinelli, R.C., "Proposed Correlation of Data for Isothermal, Two-phase, Two-component Flow in Pipes", Chem. Eng. Prog., 45, 49-58, 1949.
8. Hoogendoorn, C.J., "Gas-Liquid Flow in Horizontal Pipes", Chem. Eng. Sci., G.B., 9, 205-217, 1959.
9. Chenoweth, J.M. and Martin, M.W., "Pressure Drop Correlation for Turbulent Two-phase Flow of Gas-Liquid Mixtures in Horizontal Pipe", Pet. Ref., 34, 151-155, October, 1955.
10. Baker, O., "Design of Pipelines for Multiphase Flow of Oil and Gas", The Oil and Gas Journal, 53, 185-195, July 26, 1954.
11. Baker, O., "Multiphase Flow in Pipelines", The Oil and Gas Journal, 56, 156-167, No. 10, 1958.

12. Govier, G.W., Radford, B.A. and Dunn, J.S.C., "The Upward Vertical Flow of Air-Water Mixtures, I. Effect of Air and Water Rates on Flow Pattern, Holdup and Pressure Drop", Can. Jour. Chem. Eng. 35, 58-79, August 19, 1957.
13. Bennett, J.A.R. and Thornton, J.D., "Pressure-drop Data for the Vertical Flow of Air-Water Mixtures in the Climbing-Film and Liquid Dispersed Regions", U.K. Atomic Energy Authority, AERE-R 3195, 1959.
14. Ros, N.C.J., "Simultaneous Flow of Gas and Liquid as Encountered in Oil Wells", Koninklijke/Shell, Publication 196, April, 1960.
15. Teletov, S.G., "On the Coefficients of Resistance for the Movement of Two-phase Mixtures", Compt. Rend. Acad. Sci., U.S.S.R., 51, 579-582, 1946.
16. Wicks, M. and Dukler, A.E., "Entrainment and Pressure Drop in Concurrent Gas-Liquid Flow I. Air-Water in Horizontal Flow", A.I.Ch.E. Jour. 6, No. 3, 463, 1960.
17. Calvert, S. and Williams, B., "Upward Cocurrent Annular Flow of Air and Water in Smooth Tubes", A.I.Ch.E. Jour. 1, No. 1, 78, 1955.
18. Anderson, G.H. and Mantzouranis, B.G., "Two-phase (Gas-Liquid) Flow Phenomena I", Chem. Eng. Sci. G.B., 12, No. 3, 109-126, 1960.
19. Anderson, G.H. and Mantzouranis, B.G., "Two-phase (Gas-Liquid) Flow Phenomena II", Chem. Eng. Sci. G.B., 12, No. 4, 233, 1960.
20. Collier, J.G. and Hewitt, G.F., "Data on the Vertical Flow of Air-Water Mixtures in the Annular and Dispersed Flow Regions - B. Film Thickness and Entrainment Data and Analysis of Pressure Drop Measurements", U.K. Atomic Energy Authority, AERE-R 3455, 1960.
21. McManus, H.N. Jr., "Film Characteristics and Dimensions in Annular Two-phase Flow", Proceedings of the Sixth Midwestern Conference on Fluid Mechanics, Univ. of Texas, 1959.

A P P E N D I C E S

APPENDIX A

- (1) Composition of the Gas
- (2) Summary of Data Describing Test Section.

APPENDIX A

TABLE A-1

COMPOSITION OF THE GAS

Average composition of the gas on dry basis as supplied
by the Northwestern Utilities

<u>Component</u>	<u>Mole Percent</u>
Methane	86.18
Ethane	7.49
Propane	3.67
i-Butane	0.23
n-Butane	0.39
i-Pentane	0.17
Hydrogen Sulphide	0
Nitrogen	1.58
Carbon Dioxide	0.29

Gravity = 0.647 (Air = 1.0)

Average gravity was recorded for each day and it
varied between 0.64 and 0.66.

Water Content

Water content of the gas was measured by adsorbing the water from a measured quantity of gas on anhydrous magnesium perchlorate contained in a desiccant tube. The affinity of the desiccant for hydrocarbons is easily satisfied by passing a small amount of natural gas (1 S.C.F.*) through it. The desiccant is capable of absorbing 30 percent of its weight of water. Water content of the gas varied between 0.000724 to 0.000806 cm^3 per S.C.F.

* S.C.F. means a cu.ft. of gas at 14.4 psia and 60°F.

APPENDIX A

TABLE A-2

SUMMARY OF DATA DESCRIBING TEST SECTIONS

Measurement	One-Inch Pipe	Two-Inch Pipe
Pipe Type	Schedule 40 Aluminum Pipe	Schedule 40 Aluminum Pipe
Outside Diameter, Inches	1.315	2.375
Wall Thickness, Inches	0.133	0.154
Inside Diameter, Inches	1.049	2.067
Length of Upstream Calming Zone, ft.	24	22
Length of the Test Section, ft.	40	80
Number of Pressure Taps	5	5
Distance Between Pressure Taps, ft.	10	20
Length of Downstream Calming Section, ft.	15	20

APPENDIX B

- 1 One-Inch Pipe Experimental Data
- 2 Two-Inch Pipe Experimental Data
- 3 One-Inch Pipe Calculated Data
- 4 Two-Inch Pipe Calculated Data
- 5 One-Inch Pipe Pressure Gradient Ratio Data
- 6 Two-Inch Pipe Pressure Gradient Ratio Data
- 7 One-Inch Pipe Calculated Data Based on
Mixture Properties
- 8 Two-Inch Pipe Calculated Data Based on
Mixture Properties
- 9 Calculation of Data

T A B L E B-1

ONE-INCH EXPERIMENTAL DATA

Test Number	Gas Rate Std. ft. ³ sec.	Average Temperature °R (°F + 460)	Pressure, p.s.i.a.				Superficial Water Velocity ft. sec.
			P ₁	P ₂	P ₃ *	P ₄	
(1)	(2)	(3)	(4)	(5)	(6)	(7)	(8)
<u>Single-phase</u>							
1S	5.04	514	115.1	114.4	113.7	113.0	112.3
2S	6.25	506	115.7	114.8	113.7	112.7	111.8
3S	3.04	516	114.3	114.1	113.7	112.9	112.6
4S	21.73	497	150.8	143.2	133.7	122.3	111.9
5S	20.77	498	149.2	142.3	133.7	123.5	114.2
6S	19.77	498	148.0	140.6	133.7	124.5	116.1
7S	17.64	500	145.2	140.1	133.7	126.3	119.9
8S	9.85	510	137.7	135.9	133.7	131.5	129.5
9S	17.15	509	126.1	120.7	114	105.8	98.3
10S	14.89	509	123.1	119.0	114	108.2	103.1
11S	9.93	516	118.7	116.5	114	111.2	108.8
12S	8.66	520	117.5	115.8	114	112.0	110.2
13S	4.67	523	115.3	114.6	114	113.3	112.6
<u>Two-phase Constant Density</u>							
7X	14.95	516	156.3	145.2	133.6	121.8	108.2
8X	14.35	517	154	144.4	133.6	122.7	110.2
9X	12.50	520	150.7	142.4	133.6	125.2	115.9

70

* Mid-point Pressure

(1)	(2)	(3)	(4)	(5)	(6)	(7)	(8)	(9)
10X	5.97	532	144.2	138.9	133.6	128.2	122.8	2.42
11X	8.01	504	147.1	140.4	133.6	127.4	121.6	2.42
12X	10.69	503	148.5	141.1	133.6	126.5	119.3	2.42
13X	3.69	509	140.8	137.3	133.6	129.2	125.4	2.42
14X	5.76	510	143.8	138.8	133.6	127.8	122.4	2.42
15X	7.34	509	145.4	139.5	133.6	127.9	122.8	2.42
2X	15.8	520	157.5	146.5	133.7	120.3	103.7	1.154
4X	15.95	517	157.7	146.5	133.7	120.4	104.8	1.154
5X	12.0	525	148.8	141.6	133.7	125.7	117.1	1.154
6X	7.44	531	143.6	138.8	133.7	129.0	124.3	1.154
60	4.05	534	139.3	136.7	133.6	130.6	127.6	1.154
61	2.68	539	136.7	134.9	133.1	131.3	129.4	1.154
62	5.56	529	141.3	137.5	133.6	129.6	125.6	1.154
63	7.38	528	143.1	137.3	133.6	128.7	124.1	1.154
6	16.62	514	158.2	146.7	133.7	119.8	103.6	0.3914
7	16.42	514	157.1	145.9	133.7	120.6	105.2	0.3914
8	15.79	515	155.7	145.2	133.7	121.6	108.3	0.3914
9	15.21	516	154.4	144.5	133.7	122.4	110.2	0.3914
10	14.70	517	152.7	143.6	133.7	123.4	112.8	0.3914
11	13.50	520	149.7	141.9	133.7	125.0	116.2	0.3914
12	11.90	520	146.5	140.2	133.7	127.0	120.5	0.3914
13	8.49	525	141.5	137.6	133.7	129.8	126.4	0.3914
29	3.342	526	136.5	135.1	133.6	132.1	130.6	0.3914
30	2.321	531	134.2	133.4	132.6	131.7	131	0.3914
31	3.81	525	137.2	135.4	133.6	131.8	130.0	0.3914
32	4.86	521	138.8	136.5	134.1	131.6	129.2	0.3914
33	6.96	512	140.8	147.3	133.6	129.8	126.3	0.3914
34	6.35	513	141.0	137.9	134.6	131.3	128.3	0.3914
65	3.95	514	134.7	134.2	133.6	132.9	132.8	0.0102
68	4.72	512	135.0	134.1	133.2	132.2	131.2	0.0100
70	6.20	516	136.6	135.1	133.6	132.0	130.4	0.00970

(1)	(2)	(3)	(4)	(5)	(6)	(7)	(8)	(9)
71	7.47	512	138	135.9	133.6	131.5	129.2	0.00941
72	9.41	507	139.2	136.1	132.6	129.1	125.5	0.0090
73	12.55	510	145.5	140.3	134.6	127.1	118.8	0.0083
74	14.57	506	147.8	141.1	133.6	126.1	117.8	0.00782
75	16.25	504	151.5	143.1	133.6	124.0	113.4	0.00747
76	18.48	502	155.0	144.6	132.6	119.9	105.4	0.00694
77	19.57	503	157.5	146.0	132.6	118.9	101.9	0.00670
37	4.72	520	136.3	134.8	133.1	131.5	129.6	0.1236
38	3.86	527	135.9	134.8	133.6	132.4	131.2	0.1236
39	3.31	535	135.3	134.6	133.6	132.6	131.7	0.1236
40	2.68	538	134.7	134.2	133.6	132.9	132.2	0.1236
41	17.45	510	159.1	147.2	133.6	119.1	102.0	0.1236
42	16.65	510	157.2	146.2	133.6	120.3	104.8	0.1236
43	14.6	514	152.1	143.4	133.6	123.6	112.4	0.1236
44	12.9	518	148.2	141.3	133.6	125.9	117.6	0.1236
45	9.2	525	141.8	137.8	133.1	128.4	123.4	0.1236
46	6.5	530	138.4	136.3	133.6	131.0	128.7	0.1236
35	6.79	505	138.8	136.1	133.1	130.2	127.1	0.1236
36	5.77	510	138.1	135.9	133.6	131.2	129	0.1236
47	6.54	500	138.1	135.9	133.6	131.2	128.9	0.04561
48	9.54	516	142.2	138.2	133.6	129.1	136.2	0.04561
49	12.92	508	148.5	141.7	134.1	126.4	118.1	0.04561
50	11.6	511	145.6	139.9	133.6	127.4	120.8	0.04561
51	14.3	511	150.9	142.8	133.6	124.2	113.9	0.04561
52	15.25	509	153.3	144.1	133.6	122.7	110.7	0.04561
53	16.2	505	156.3	146.0	134.1	121.5	107.2	0.04561
54	17.3	503	157.9	146.6	133.6	119.7	103.4	0.04561
55	17.9	504	159.3	147.4	133.6	118.8	101.0	0.04561
56	3.67	523	135.8	134.9	134.1	133.2	132.6	0.04561
57	4.88	521	136.3	134.8	133.6	132.2	130.9	0.04561
58	1.96	533	134.0	133.8	133.6	133.4	133.2	0.04561
59	3.09	528	133.7	133.0	132.6	131.9	131.5	0.04561

(1)	(2)	(3)	(4)	(5)	(6)	(7)	(8)	(9)
<u>Two-phase Variable Density</u>								
14	18.25	510	164.1	152.2	138.7	124.2	108.0	0.3914
15	16.25	510	148.3	137.2	125.2	112.2	97.4	0.3914
16	14.41	515	133.1	123.1	112.2	100.4	87.4	0.3914
17	12.22	513	113.7	105.4	96.2	86.4	75.4	0.3914
18	10.78	520	100.2	92.8	84.7	76.0	66.6	0.3914
19	9.48	516	88.0	81.7	74.7	67.1	58.7	0.3914
20	7.32	519	70.2	65.1	59.7	53.9	47.6	0.3914
21	5.56	520	54.4	50.7	46.7	42.4	37.7	0.3914
22	4.36	527	48.8	46.1	42.7	39.2	35.5	0.3914

T A B L E B-2

TWO-INCH PIPE EXPERIMENTAL DATA

Test Number	Gas Rate Std. ft. ³ sec.	Average Temperature °R (°F + 460)	P ₃ [*] p.s.i.a.	ΔP inches H ₂ O $\frac{\Delta P}{80 \text{ ft. length}}$	Superficial Water Velocity $\frac{\text{ft.}}{\text{sec.}}$
(1)	(2)	(3)	(4)	(5)	(6)
<u>Single-phase</u>					
1S	30.84	498	139.6	132	-
2S	29.12	498	133.6	125.4	-
3S	30.33	495	133.6	136.5	-
4S	26.31	505	133.6	103	-
5S	22.2	504	133.6	74	-
6S	18.15	508	133.6	52.5	-
7S	14.87	513	133.1	36	-
8S	10.26	517	133.6	19	-
9S	5.46	519	133.1	5.5	-
10S	6.55	517	132.1	8.5	-
<u>Two-phase Constant Density</u>					
22	23.79	510	133.6	328	0.525
23	20.77	516	133.1	280	0.525
24	17.95	523	133.6	228	0.525

* Mid-point Pressure

(1)	(2)	(3)	(4)	(5)	(6)
25	15.88	527	133.6	190	0.525
26	12.58	529	133.6	130	0.525
27	10.62	530	133.6	96.5	0.525
40	12.40	531	131.6	123.0	0.525
41	12.61	531	133.1	126.5	0.525
42	10.61	533	133.6	93.5	0.525
43	7.63	531	133.6	46	0.525
44	5.33	530	131.6	29.5	0.525
28	11.77	530	133.6	93	0.293
29	14.19	525	133.6	139	0.293
30	16.33	522	133.6	179	0.293
31	19.15	519	133.6	230	0.293
32	21.67	518	133.6	262	0.293
33	24.16	517	133.6	306	0.293
34	26.92	515	133.1	344	0.293
35	28.97	515	133.6	388	0.293
36	7.31	526	133.6	33	0.293
37	9.25	531	134.1	54	0.293
38	11.32	517	132.6	86.0	0.293
39	13.79	523	133.6	128.5	0.293
50	15.71	494	133.6	97.5	2.87
51	9.79	513	133.6	22	3.13
52	7.79	514	134.1	16	3.43
53	16.61	506	134.6	68	3.24
54	18.65	503	134.1	90	2.83
55	20.86	498	132.6	112.5	2.79
56	24.29	496	133.6	154	2.68
57	34.30	395	133.6	178.5	2.34

(1)	(2)	(3)	(4)	(5)	(6)
58	24.25	509	132.6	244	0.1
59	26.69	503	133.6	288	0.1
60	28.55	500	133.6	320	0.1
61	31.60	496	133.6	392	0.1
62	29.77	500	133.6	350	0.1
63	27.23	501	133.6	296	0.1
64	24.63	505	133.6	256	0.1
65	21.56	508	134.6	206	0.1
66	20.34	511	133.6	183	0.1
67	18.32	514	133.6	159	0.1
68	16.79	517	134.1	138	0.1
69	17.25	517	133.6	144.5	0.1
70	14.14	521	134.1	103	0.1
71	15.37	521	134.1	120.5	0.1
72	12.84	520	133.6	84	0.1
73	10.38	525	132.6	48	0.1
74	11.51	527	133.6	64.5	0.1
75	8.87	530	133.6	34	0.1
76	7.86	533	134.6	26.5	0.1
77	6.69	530	134.6	17.0	0.1
78	4.90	526	132.6	10.5	0.1
79	4.04	515	132.6	3.2	0.00303
80	5.38	511	134.1	7.4	0.00303
81	7.29	507	133.6	12	0.00303
82	9.03	511	133.6	16.6	0.00303
83	10.32	513	134.1	22	0.00303
84	11.79	510	134.6	27.5	0.00303
85	12.93	505	134.1	33	0.00303
86	15.05	507	133.6	47.5	0.00303

(1)	(2)	(3)	(4)	(5)	(6)
87	15.99	505	133.6	57.5	0.00303
88	18.07	500	133.6	75	0.00303
89	19.31	501	133.6	85	0.00303
90	19.44	505	133.6	86	0.00303
91	21.01	500	133.6	105.6	0.00303
92	22.81	498	133.1	127.5	0.00303
93	25.02	495	133.6	153	0.00303
94	21.21	502	133.1	166	0.0318
95	19.96	503	133.6	145.5	0.0318
96	18.30	506	133.6	125	0.0318
97	16.85	510	133.6	101	0.0318
98	17.01	509	133.6	84	0.01215
99	17.56	509	133.6	93	0.01215
100	19.62	505	133.6	117	0.01215
101	21.77	504	133.6	142	0.01215
102	23.64	497	132.6	172.5	0.01215
103	6.59	501	133.6	10.5	0.01215
104	8.59	503	133.6	20	0.01215
105	10.14	503	132.6	27	0.01215
106	12.99	511	133.6	44	0.01215
107	11.52	515	133.1	35	0.01215
108	14.22	509	133.6	61	0.01215
109	16.17	506	133.6	76.5	0.01215
110	18.95	506	133.6	136.7	0.0318
111	17.84	509	133.6	123.5	0.0318
112	16.34	511	133.6	100.5	0.0318
113	15.23	509	133.6	89	0.0318
114	13.31	510	134.1	63.5	0.0318
115	11.48	515	133.6	48.5	0.0318

(1)	(2)	(3)	(4)	(5)	(6)
116	10.29	511	133.6	34.7	0.0318
117	9.11	511	133.6	29	0.0318
118	8.23	513	133.6	23	0.0318
119	7.37	516	133.6	15.5	0.0318
<u>Two-phase Variable Density</u>					
140	28.18	499	172.5	286	0.293
141	26.66	499	163.5	280	0.293
142	24.87	500	153.5	268	0.293
143	23.74	501	147	260	0.293
144	21.64	502	133.5	246	0.293
145	18.59	504	116.5	224	0.293
146	16.42	505	103.5	200	0.293
147	14.42	506	91.5	184	0.293
148	12.90	508	82.5	164	0.293
149	11.16	510	72	152	0.293
150	9.85	510	63.5	134	0.293
151	8.27	510	54.5	120	0.293
152	6.25	511	42.5	89	0.293
153	4.70	511	32.5	70	0.293
120	31.65	492	177.5	272	0.0318
121	29.56	493	165.5	252	0.0318
122	26.65	494	150.5	228	0.0318
123	24.83	495	140	212	0.0318
124	23.18	496	130.5	196	0.0318
125	21.62	496	122	186	0.0318
126	19.20	497	109.5	165	0.0318

(1)	(2)	(3)	(4)	(5)	(6)
127	16.63	498	95.5	146	0.0318
128	14.30	500	81.5	127	0.0318
129	12.63	502	71.5	114	0.0318
130	10.74	505	61.5	97	0.0318
131	9.25	506	51.5	83	0.0318
132	7.35	506	41	64	0.0318
133	5.31	506	29.5	45	0.0318

T A B L E B-3

ONE-INCH PIPE CALCULATED DATA

Test Number	Gas Density $\frac{\text{lbs.}}{\text{ft.}^3}$	Superficial Gas Velocity $\frac{\text{ft.}}{\text{sec.}}$	Superficial Water Velocity $\frac{\text{ft.}}{\text{sec.}}$	$\left(\frac{dP}{dL}\right)^*$ $\frac{\text{lbs.}}{\text{ft.}^2}$ per $\frac{\text{ft.}}{\text{ft.}^2}$	$\left(\frac{dP}{dL}\right)$ (Adjusted to 0.47 $\frac{\text{lbs.}}{\text{ft.}^3}$ gas density)
(1)	(2)	(3)	(4)	(5)	(6)
<u>Single-phase</u>					
1S	0.401	102.29	-	9.43	11.02
2S	0.407	124.71	-	14.58	16.8
3S	0.399	61.84	-	7.74	9.7
4S	0.488	362.07	-	142.20	137
5S	0.487	346.79	-	135.36	130.8
6S	0.487	330.09	-	124.2	120
7S	0.485	295.74	-	97.92	94.8
8S	0.475	168.43	-	31.50	31.1
9S	0.406	343.29	-	109.08	126.2
10S	0.406	298.05	-	78.12	90.4
11S	0.400	201.60	-	38.34	44
12S	0.397	177.09	-	27.47	32.5
13S	0.395	96.03	-	9.54	11.34

* At experimental mid-point conditions

(1)	(2)	(3)	(4)	(5)	(6)
<u>Two-phase Constant Density</u>					
7X	0.469	258.80	2.42	169.20	169.6
8X	0.468	248.89	2.42	154.8	154.8
9X	0.466	218.06	2.42	122.4	123.4
10X	0.455	106.54	2.42	76.79	79.4
11X	0.481	135.43	2.42	93.6	91.7
12X	0.481	180.41	2.42	104.76	102
13X	0.476	63.00	2.42	56.88	56
14X	0.475	98.56	2.42	78.84	77.9
15X	0.476	125.33	2.42	84.60	83.6
2X	0.466	275.52	1.154	163.8	165
4X	0.469	276.53	1.154	160.92	160.92
5X	0.462	211.25	1.154	109.80	111.8
6X	0.456	132.49	1.154	70.13	72.3
60	0.453	72.58	1.154	42.48	44
61	0.447	48.66	1.154	25.99	27.25
62	0.458	98.71	1.154	57.24	58.8
63	0.465	129.00	1.154	68.40	69.4
6	0.471	286.50	0.3914	194.4	194.0
7	0.471	283.05	0.3914	181.08	180.5
8	0.470	272.71	0.3914	171.36	171
9	0.470	263.20	0.3914	159.84	159.89
10	0.469	254.86	0.3914	145.44	145.4
11	0.466	235.41	0.3914	120.60	121.3
12	0.466	207.51	0.3914	94.32	94.7
13	0.462	149.46	0.3914	55.62	56.5
29	0.460	58.99	0.3914	21.49	21.7

(1)	(2)	(3)	(4)	(5)	(6)
30	0.453	41.66	0.3914	11.59	11.72
31	0.461	67.11	0.3914	25.92	26.4
32	0.467	84.64	0.3914	34.74	35
33	0.473	119.57	0.3914	52.74	52.4
34	0.476	108.50	0.3914	47.34	46.6
65	0.471	68.11	0.0102	4.61	4.6
68	0.470	81.64	0.0100	13.82	13.82
70	0.469	107.33	0.00970	22.36	22.36
71	0.473	128.33	0.00941	31.86	31.63
72	0.474	161.29	0.0090	50.40	49.92
73	0.478	213.13	0.0083	95.4	93.63
74	0.479	247.38	0.00782	108.36	106.59
75	0.480	274.82	0.00747	137.52	134.40
76	0.479	313.64	0.00694	178.20	174.78
77	0.478	332.76	0.00670	195.12	191.73
37	0.464	82.64	0.1236	24.12	24.4
38	0.460	68.25	0.1236	25.2	25.75
39	0.453	59.41	0.1236	13.78	14.3
40	0.450	48.37	0.1236	9.11	9.52
41	0.475	298.60	0.1236	203.04	193.2
42	0.475	284.90	0.1236	186.48	182.8
43	0.471	251.78	0.1236	142.56	141.8
44	0.468	224.18	0.1236	110.88	111.5
45	0.461	162.06	0.1236	67.32	68.5
46	0.457	115.57	0.1236	37.8	38.8
35	0.478	115.45	0.1236	42.77	42.0
36	0.475	98.73	0.1236	35.64	34.82

(1)	(2)	(3)	(4)	(5)	(6)
47	0.484	109.69	0.04561	33.73	32.6
48	0.469	165.15	0.04561	65.88	65.88
49	0.479	219.37	0.04561	109.44	108.4
50	0.474	198.86	0.04561	100.94	100.1
51	0.474	245.15	0.04561	133.92	132.8
52	0.476	260.39	0.04561	153.72	152
53	0.481	273.40	0.04561	176.4	172
54	0.482	291.9	0.04561	194.4	189.5
55	0.481	302.7	0.04561	204.48	200
56	0.465	64.14	0.04561	12.13	12.28
57	0.465	85.29	0.04561	19.62	19.85
58	0.454	35.04	0.04561	2.92	3.02
59	0.455	55.14	0.04561	8.60	8.89

Two-phase Variable Density

14	0.493	300.8	0.3914	201.24	-
15	0.445	296.72	0.3914	180	-
16	0.395	296.47	0.3914	163.8	-
17	0.340	292.14	0.3914	136.4	-
18	0.295	296.70	0.3914	120.24	-
19	0.262	293.60	0.3914	103.68	-
20	0.208	285.26	0.3914	81.36	-
21	0.162	277.59	0.3914	58.25	-
22	0.147	241.22	0.3914	49.32	-

T A B L E B-4

TWO-INCH CALCULATED DATA

Test Number	Gas Density $\frac{\text{lbs.}}{\text{ft}^3}$	Superficial Gas Velocity $\frac{\text{ft.}}{\text{sec.}}$	Superficial Water Velocity $\frac{\text{ft.}}{\text{sec.}}$	$\left(\frac{dP}{dL}\right)^*$ $\frac{\text{lbs.}}{\text{ft}^2}$ per ft.	$\left(\frac{dP}{dL}\right)$ (Adjusted to 0.47 $\frac{\text{lbs.}}{\text{ft}^3}$ gas density)
(1)	(2)	(3)	(4)	(5)	(6)
<u>Single-phase</u>					
1S	0.508	127.20	-	8.58	7.94
2S	0.486	125.55	-	8.15	7.87
3S	0.489	129.93	-	8.87	8.52
4S	0.480	115.01	-	6.69	6.56
5S	0.480	96.77	-	4.81	4.71
6S	0.477	79.67	-	3.41	3.36
7S	0.475	65.63	-	2.34	2.31
8S	0.468	45.92	-	1.23	1.24
9S	0.465	24.63	-	0.35	0.35
10S	0.463	29.65	-	0.55	0.56

* At experimental mid-point conditions

(1)	(2)	(3)	(4)	(5)	(6)
<u>Two-Phase Constant Density</u>					
22	0.475	105.07	0.525	21.33	21.18
23	0.467	93.13	0.525	18.20	18.21
24	0.463	81.91	0.525	14.82	14.6
25	0.459	72.44	0.525	12.35	12.49
26	0.458	57.60	0.525	8.45	8.54
27	0.457	48.73	0.525	6.27	6.33
40	0.449	57.86	0.525	7.99	8.16
41	0.454	58.18	0.525	8.22	8.34
42	0.454	48.94	0.525	6.08	6.16
43	0.456	35.08	0.525	2.99	3.02
44	0.450	24.81	0.525	1.91	1.93
28	0.457	54.00	0.293	6.04	6.14
29	0.463	64.24	0.293	9.03	9.12
30	0.464	73.78	0.293	11.64	11.73
31	0.467	86.01	0.293	14.95	14.96
32	0.467	97.17	0.293	17.03	17.04
33	0.468	108.14	0.293	19.89	19.90
34	0.463	121.86	0.293	22.37	22.61
35	0.470	129.17	0.293	25.23	25.23
36	0.360	33.28	0.293	2.14	2.16
37	0.458	42.37	0.293	3.51	3.55
38	0.465	51.02	0.293	5.59	5.62
39	0.463	62.44	0.293	8.35	8.44
50	0.490	67.18	2.87	6.34	
51	0.472	43.47	3.13	1.43	
52	0.473	34.42	3.43	1.04	

(1)	(2)	(3)	(4)	(5)	(6)
53	0.482	72.21	3.24	4.42	
54	0.483	80.90	2.83	5.85	
55	0.483	90.61	2.79	7.31	
56	0.488	104.30	2.68	10.01	
57	0.489	146.99	2.34	11.28	
58	0.472	107.65	0.1	15.86	15.79
59	0.481	116.22	0.1	18.72	18.32
60	0.484	123.57	0.1	20.81	20.23
61	0.488	135.66	0.1	25.49	24.60
62	0.484	128.85	0.1	22.76	22.13
63	0.483	118.1	0.1	19.24	18.75
64	0.479	107.69	0.1	16.64	16.34
65	0.480	94.10	0.1	13.39	13.10
66	0.474	90.00	0.1	11.90	11.80
67	0.471	81.52	0.1	10.34	10.31
68	0.470	74.86	0.1	8.97	8.97
69	0.468	77.20	0.1	9.39	9.41
70	0.466	63.53	0.1	6.69	6.73
71	0.466	69.05	0.1	7.83	7.87
72	0.466	57.79	0.1	5.46	5.49
73	0.461	47.18	0.1	3.12	3.16
74	0.459	52.50	0.1	4.19	4.26
75	0.457	40.68	0.1	2.21	2.25
76	0.458	36.02	0.1	1.72	1.75
77	0.460	30.46	0.1	1.10	1.12
78	0.457	22.49	0.1	0.68	0.69
79	0.467	17.13	0.00303	0.20	0.20
80	0.476	23.7	0.00303	0.48	0.47

(1)	(2)	(3)	(4)	(5)	(6)
81	0.478	32.0	0.00303	0.78	0.76
82	0.474	39.92	0.00303	1.08	1.07
83	0.474	45.64	0.00303	1.43	1.41
84	0.478	51.66	0.00303	1.78	1.75
85	0.481	56.32	0.00303	2.14	2.09
86	0.478	66.06	0.00303	3.08	3.03
87	0.480	69.88	0.00303	3.73	3.65
88	0.484	78.20	0.00303	4.87	4.72
89	0.483	83.74	0.00303	5.52	5.36
90	0.480	84.96	0.00303	5.59	4.91
91	0.484	90.92	0.00303	6.86	6.65
92	0.485	98.69	0.00303	8.28	9.64
93	0.489	107.18	0.00303	9.94	9.96
94	0.481	92.49	0.0318	10.79	10.55
95	0.481	86.89	0.0318	9.46	9.23
96	0.479	80.13	0.0318	8.13	7.98
97	0.475	74.39	0.0318	6.56	6.49
98	0.476	74.95	0.01215	5.46	5.38
99	0.476	77.34	0.01215	6.04	5.96
100	0.480	85.78	0.01215	7.60	7.44
101	0.481	94.97	0.01215	9.29	9.08
102	0.484	102.43	0.01215	11.21	10.89
103	0.483	28.56	0.01215	0.68	0.66
104	0.481	37.38	0.01215	1.3	1.76
105	0.478	44.50	0.01215	1.75	1.72
106	0.474	57.46	0.01215	2.86	2.83
107	0.468	51.57	0.01215	2.27	2.28
108	0.476	62.66	0.01215	3.96	3.91
109	0.479	70.82	0.01215	4.97	4.88

(1)	(2)	(3)	(4)	(5)	(6)
110	0.479	82.98	0.0318	8.88	8.72
111	0.476	78.57	0.0318	8.02	7.92
112	0.474	72.27	0.0318	6.53	6.47
113	0.476	67.09	0.0318	5.78	5.71
114	0.477	58.52	0.0318	4.12	4.08
115	0.470	51.16	0.0318	3.15	3.14
116	0.474	45.52	0.0318	2.25	2.23
117	0.474	40.29	0.0318	1.88	1.86
118	0.472	36.52	0.0318	1.49	1.48
119	0.469	32.92	0.0318	1.00	1.00

Two-phase Variable Density

140	0.634	93.18	0.293	18.59	7.79
141	0.600	93.2	0.293	18.20	5.55
142	0.561	92.99	0.293	17.42	4.87
143	0.535	93.06	0.293	16.90	5.00
144	0.483	93.88	0.293	15.99	4.6
145	0.419	93.08	0.293	14.56	4.05
146	0.370	93.00	0.293	13.00	3.62
147	0.325	92.85	0.293	11.96	3.26
148	0.292	92.68	0.293	10.66	2.98
149	0.253	92.54	0.293	9.88	2.62
150	0.222	92.88	0.293	8.71	2.36
151	0.190	91.13	0.293	7.80	1.99
152	0.147	88.72	0.293	5.78	1.54
153	0.112	87.33	0.293	4.55	1.18

(1)	(2)	(3)	(4)	(5)	(6)
120	0.663	100.06	0.0318	17.68	6.94
121	0.615	100.75	0.0318	16.38	6.47
122	0.556	100.40	0.0318	14.82	5.93
123	0.515	101.07	0.0318	13.78	5.54
124	0.478	101.65	0.0318	12.74	5.28
125	0.446	101.63	0.0318	12.09	4.95
126	0.398	101.16	0.0318	10.72	4.54
127	0.345	100.89	0.0318	9.49	3.97
128	0.292	102.46	0.0318	8.25	3.62
129	0.255	103.79	0.0318	7.41	3.15
130	0.217	103.45	0.0318	6.30	2.74
131	0.181	106.92	0.0318	5.39	2.5
132	0.144	106.93	0.0318	4.16	2.05
133	0.103	107.74	0.0318	2.92	1.6

T A B L E B-5

ONE-INCH PIPE PRESSURE GRADIENT RATIO DATA

Superficial Water Velocity $\frac{\text{ft.}}{\text{sec.}}$	Superficial Gas Velocity $\frac{\text{ft.}}{\text{sec.}}$	$\frac{dP}{dL}$ $\frac{\text{lbs.}}{\text{ft.}^2}$ per ft.	$\frac{dP}{dL} / \left(\frac{dP}{dL}\right)_g$	Friction Factor Based on Gas Properties f_{tpg}
(1)	(2)	(3)	(4)	(5)
0.01	30	1.36	1.096	0.00444
0.01	40	2.95	1.38	0.00518
0.01	50	4.99	1.55	0.00597
0.01	60	7.5	1.65	0.00623
0.01	70	10.3	1.695	0.00629
0.01	80	13.5	1.722	0.00613
0.01	90	17	1.74	0.00628
0.01	100	20.5	1.71	0.00614
0.01	120	29.5	1.735	0.00613
0.01	140	40	1.775	0.00611
0.01	180	67	1.84	0.00619
0.01	200	84	1.9	0.00628
0.01	220	98.5	1.82	0.00609
0.01	250	124	1.785	0.00594
0.01	300	175	1.785	

(1)	(2)	(3)	(4)	(5)
0.03	30	1.8	1.45	0.00599
0.03	40	3.7	1.73	0.00692
0.03	50	6.35	1.98	0.00760
0.03	60	9.4	2.06	0.00781
0.03	70	13.1	2.22	0.00800
0.03	80	17	2.17	0.00795
0.03	90	21	2.15	0.00776
0.03	100	25.2	2.1	0.00754
0.03	120	35.8	2.11	0.00693
0.03	140	46	2.04	0.00703
0.03	180	73	2	0.00674
0.03	200	89	2.01	0.00666
0.03	220	106	1.96	0.00655
0.03	250	134	1.93	0.00642
0.03	300	193	1.98	
0.10	30	3.03	2.44	0.01005
0.10	40	5.85	2.73	0.01095
0.10	50	9.4	2.93	0.01124
0.10	60	13.4	2.94	0.01137
0.10	70	17.9	2.95	0.01093
0.10	80	22.6	2.88	0.01057
0.10	90	27.2	2.78	0.01005
0.10	100	32	2.67	0.00958
0.10	120	42.6	2.51	0.00885
0.10	140	52.5	2.33	0.00801
0.10	180	78.6	2.16	0.00726
0.10	200	94	2.12	0.00703
0.10	220	111	2.05	0.00686

(1)	(2)	(3)	(4)	(5)
0.10	250	141	2.03	0.00676
0.10	300	200	2.04	
0.30	30	5.4	4.35	0.0180
0.30	40	9.6	4.49	0.0180
0.30	50	14.4	4.48	0.0172
0.30	60	19.5	4.28	0.0162
0.30	70	24.9	4.1	0.0152
0.30	80	30.3	3.87	0.0142
0.30	90	35.2	3.6	0.0130
0.30	100	40.1	3.35	0.0120
0.30	120	50	2.94	0.0104
0.30	140	59.2	2.63	0.00904
0.30	180	84	2.31	0.00776
0.30	200	97	2.19	0.00725
0.30	220	113	2.09	0.00699
0.30	250	145	2.08	0.00695
0.30	300	205	2.09	
1.00	30	11.7	9.44	0.0372
1.00	40	18.7	8.74	0.0350
1.00	50	25.7	8	0.0308
1.00	60	32.9	7.22	0.0274
1.00	70	39	6.42	0.0238
1.00	80	45.9	5.85	0.0215
1.00	90	50.8	5.2	0.0188
1.00	100	55.2	4.61	0.0165
1.00	120	64.1	3.77	0.0133
1.00	140	72	3.2	0.0110

(1)	(2)	(3)	(4)	(5)
1.00	180	93	2.55	0.00859
1.00	200	105	2.37	0.00785
1.00	220	121	2.24	0.00748
1.00	250	152	2.18	0.00728
1.00	300	212	2.16	
3.00	30	32.8	26.4	0.10907
3.00	40	44.3	20.2	0.0790
3.00	50	53.5	16.65	0.0640
3.00	60	62.0	13.6	0.0516
3.00	70	70	11.52	0.0428
3.00	80	75.5	9.64	0.0353
3.00	90	80	8.2	0.0296
3.00	100	84.5	7.5	0.0253
3.00	120	91	5.25	0.0189
3.00	140	97	4.3	0.0148
3.00	180	109	2.99	0.0101
3.00	200	115	2.6	0.00860
3.00	220	132	2.44	0.00825
3.00	250	158	2.27	0.00756
3.00	300	219	2.23	

T A B L E B-6

TWO-INCH PIPE PRESSURE GRADIENT RATIO DATA

Superficial Water Velocity $\frac{\text{ft.}}{\text{sec.}}$	Superficial Gas Velocity $\frac{\text{ft.}}{\text{sec.}}$	$\left(\frac{dP}{dL}\right)$ $\frac{\text{lbs.}}{\text{ft.}^2} \text{ per ft.}$	$\left(\frac{dP}{dL}\right) / \left(\frac{dP}{dL}\right)_g$	Friction Factor Based on Gas Properties f_{tpg}
(1)	(2)	(3)	(4)	(5)
0.001	25	0.46	1.155	
0.001	30	0.622	1.13	
0.001	40	0.986	1.053	
0.001	50	1.45	1.031	
0.001	60	2.12	1.08	
0.001	70	3.06	1.17	
0.001	80	4.15	1.235	
0.001	90	5.5	1.315	
0.001	100	7	1.38	
0.001	120	9.5	1.32	
0.003	25	0.495	1.242	
0.003	30	0.67	1.215	
0.003	40	1.09	1.162	
0.003	50	1.63	1.16	
0.003	60	2.49	1.27	

(1)	(2)	(3)	(4)	(5)
0.003	70	3.7	1.415	
0.003	80	5	1.488	
0.003	90	6.5	1.555	
0.003	100	8.1	1.595	
0.003	120	10.9	1.51	
0.010	25	0.576	1.45	
0.010	30	0.78	1.415	
0.010	40	1.31	1.40	
0.010	50	2.12	1.51	
0.010	60	3.3	1.67	
0.010	70	4.7	1.8	
0.010	80	6.25	1.86	
0.010	90	8	1.91	
0.010	100	9.7	1.91	
0.010	120	12.9	1.79	
0.030	25	0.69	1.732	
0.030	30	0.93	1.69	
0.030	40	1.66	1.77	
0.030	50	2.82	2.01	
0.030	60	4.33	2.2	
0.030	70	5.99	2.29	
0.030	80	7.8	2.32	
0.030	90	9.76	2.34	
0.030	100	11.75	2.31	
0.030	120	15.25	2.12	

(1)	(2)	(3)	(4)	(5)
0.10	25	0.89	2.236	
0.10	30	1.22	2.22	
0.10	40	2.27	2.423	
0.10	50	3.95	2.81	
0.10	60	5.95	3.02	
0.10	70	7.9	3.02	
0.10	80	10.15	3.02	
0.10	90	12.4	2.96	
0.10	100	14.5	2.85	
0.10	120	18.6	2.58	
0.30	25	1.2	3.015	
0.30	30	1.7	3.08	
0.30	40	3.25	3.47	
0.30	50	5.45	3.88	
0.30	60	8	4.06	
0.30	70	10.5	4.01	
0.30	80	13	3.86	
0.30	90	15.5	3.71	
0.30	100	17.8	3.5	
0.30	120	22.5	3.12	
1.0	25	1.8	4.52	
1.0	30	2.79	5.06	
1.0	40	4.9	5.24	
1.0	50	7.9	5.62	
1.0	60	11.2	5.7	
1.0	70	14.7	5.63	
1.0	80	17.3	5.14	
1.0	90	20	4.79	
1.0	100	22.6	4.45	
1.0	120	28	3.88	

T A B L E B-7

ONE-INCH PIPE CALCULATED DATA BASED ON MIXTURE PROPERTIES

Input Gas-Liquid Volume Ratio R_v	Superficial Gas Velocity V_g ft./sec.	$\frac{dP}{dL}$ lbs. ft. ² per ft.	Reynolds Number Based on Mixture Properties Re_m	Friction Factor Based on Mixture Properties f_{tpm}
(1)	(2)	(3)	(4)	(5)
50	30	8.2	186,000	0.00727
50	40	16.0	248,000	0.00799
50	50	25.7	310,000	0.00821
50	60	36.0	372,000	0.00799
50	70	45.5	434,000	0.00741
50	80	55.5	496,000	0.00692
50	90	63.0	559,000	0.00621
50	100	71.0	621,000	0.00567
50	120	84.0	745,000	0.00466
50	140	96.0	869,000	0.00391
100	30	5.4	183,000	0.00763
100	40	11.2	245,000	0.00891
100	50	18.0	306,000	0.00916
100	60	25.9	367,000	0.00916
100	70	34.0	429,000	0.00883
100	80	42.0	490,500	0.00836

(1)	(2)	(3)	(4)	(5)
100	90	49.0	551,000	0.00770
100	100	55.3	613,000	0.00704
100	120	67.2	735,000	0.00594
100	140	75.3	858,000	0.00489
100	180	100.0	1,103,000	0.00393
100	200	110.0	1,226,000	0.00350
100	220	129.0	1,348,000	0.00339
100	250	155.0	1,532,000	0.00316
100	300	219.0	1,839,000	0.00310
200	30	3.7	182,000	0.00737
200	40	7.95	243,000	0.00891
200	50	13.3	304,000	0.00953
200	60	19.5	365,000	0.00971
200	70	26.2	426,000	0.00959
200	80	33.5	487,000	0.00939
200	90	39.5	548,000	0.00874
200	100	45.5	608,000	0.00815
200	120	57.5	730,800	0.00716
200	140	67.0	852,000	0.00613
200	180	92.0	1,096,000	0.00508
200	200	105.0	1,218,000	0.00470
200	220	121.0	1,339,000	0.00448
200	250	152.0	1,522,000	0.00436
200	300	215.0	1,827,000	0.00428
400	30	2.65	182,000	0.00670
400	40	5.85	242,000	0.00820
400	50	10.2	303,000	0.00915

(1)	(2)	(3)	(4)	(5)
400	60	15.3	364,000	0.00955
400	70	21.0	424,000	0.00961
400	80	27.4	485,000	0.0097
400	90	32.8	546,000	0.00908
400	100	38.8	606,000	0.00873
400	120	50.0	728,000	0.00778
400	140	60.0	849,000	0.00686
400	180	86.5	1,092,000	0.00598
400	200	100.0	1,213,000	0.00560
400	220	115.0	1,335,000	0.00532
400	250	150.0	1,517,000	0.00538
400	300	210.0	1,821,000	0.00524
1,000	30	1.8	181,000	0.00528
1,000	40	4.0	242,000	0.00661
1,000	50	7.4	302,000	0.00781
1,000	60	11.5	363,000	0.00843
1,000	70	16.2	424,000	0.00873
1,000	80	21.4	484,000	0.00882
1,000	90	26.5	545,000	0.00863
1,000	100	32.0	605,000	0.00845
1,000	120	43.6	726,000	0.00798
1,000	140	54.5	848,000	0.00734
1,000	180	81.2	1,090,000	0.00661
1,000	200	95.0	1,211,000	0.00627
1,000	220	110.1	1,322,000	0.00605
1,000	250	145.0	1,514,000	0.00612
1,000	300	205.0	1,817,000	0.00607

(1)	(2)	(3)	(4)	(5)
2,000	30	1.48	181,000	0.00462
2,000	40	3.32	242,000	0.00583
2,000	50	6.05	302,000	0.00679
2,000	60	9.4	363,000	0.00734
2,000	70	13.6	423,000	0.00780
2,000	80	18.2	484,000	0.00799
2,000	90	32.0	544,000	0.00798
2,000	100	28.0	605,000	0.00787
2,000	120	39.5	726,000	0.00771
2,000	140	51.0	847,000	0.00731
2,000	180	78.0	1,089,000	0.00676
2,000	200	94.0	1,210,000	0.00661
2,000	220	110.5	1,331,000	0.00639
2,000	250	114.2	1,513,000	0.00513
2,000	300	200.2	1,816,000	0.00625
4,000	30	1.3	181,000	0.00418
4,000	40	2.95	242,000	0.00535
4,000	50	5.19	302,000	0.00602
4,000	60	8.10	363,000	0.00652
4,000	70	11.5	423,000	0.00680
4,000	80	15.5	484,000	0.00703
4,000	90	19.8	544,000	0.00709
4,000	100	24.5	605,000	0.00711
4,000	120	35.8	726,000	0.00741
4,000	140	47.0	847,000	0.00695
4,000	180	75.0	1,089,000	0.00671
4,000	200	91.0	1,210,000	0.00659
4,000	220	110.0	1,331,000	0.00659

(1)	(2)	(3)	(4)	(5)
4,000	250	138.0	1,512,000	0.00640
4,000	300	199.0	1,815,000	0.00641
10,000	30	1.19	181,000	0.00391
10,000	40	2.70	242,000	0.00498
10,000	50	4.45	302,000	0.00526
10,000	60	6.90	363,000	0.00566
10,000	70	9.80	423,000	0.00591
10,000	80	13.0	484,000	0.00600
10,000	90	17.0	544,000	0.00620
10,000	100	20.5	605,000	0.00606
10,000	120	31.2	726,000	0.00640
10,000	140	41.8	847,000	0.00630
10,000	180	70.0	1,089,000	0.00638
10,000	200	88.0	1,210,000	0.00650
10,000	220	104.0	1,331,000	0.00635
10,000	250	132.0	1,512,000	0.00624
10,000	300	193.0	1,815,000	0.00634
100,000	30	1.12	181,000	0.00371
100,000	40	2.2	242,000	0.00409
100,000	50	3.56	302,000	0.00424
100,000	60	5.2	363,000	0.00431
100,000	70	7.4	423,000	0.00450
100,000	80	9.7	484,000	0.00452
100,000	90	12.6	544,000	0.00464
100,000	100	16	605,000	0.00477
100,000	120	23.8	726,000	0.00492

(1)	(2)	(3)	(4)	(5)
100,000	140	32.5	847,000	0.00494
100,000	180	55	1,089,000	0.00506
100,000	200	68.5	1,210,000	0.00510
100,000	220	83	1,331,000	0.00511
100,000	250	109	1,512,000	0.00520
100,000	300	156	1,815,000	0.00516

T A B L E B-8

TWO-INCH PIPE CALCULATED DATA BASED ON MIXTURE PROPERTIES

Input Gas-Liquid Volume Ratio R_v	Superficial Gas Velocity V_g ft./sec.	$\left(\frac{dP}{dL}\right)$ $\frac{\text{lbs.}}{\text{ft}^2}$ per ft.	Reynolds Number Based on Mixture Properties Re_m	Friction Factor Based on Mixture Properties f_{tpm}
(1)	(2)	(3)	(4)	(5)
40	25	1.38	308,000	0.00294
40	30	2.22	369,000	0.00314
40	40	4.95	492,000	0.00412
40	50	7.90	616,000	0.00421
100	25	1.14	302,000	0.00387
100	30	1.70	362,000	0.00401
100	40	3.55	483,000	0.00470
100	50	6.40	603,000	0.00543
100	60	9.90	724,000	0.00584
100	70	13.30	846,000	0.00577
100	80	16.40	966,000	0.00544
100	90	19.60	1,088,000	0.00514
100	100	22.60	1,206,000	0.00479
100	120		1,450,000	

(1)	(2)	(3)	(4)	(5)
200	25	0.945	302,000	0.00534
200	30	1.370	360,000	0.00536
200	40	2.84	481,000	0.00627
200	50	5.15	601,000	0.00727
200	60	8.00	720,000	0.00785
200	70	10.90	840,000	0.00786
200	80	13.90	960,000	0.00766
200	90	16.80	1,081,000	0.00732
200	100	19.60	1,200,000	0.00692
200	120	25.4	1,440,000	0.00622
400	25	0.8	301,000	0.00566
400	30	1.13	359,000	0.00555
400	40	2.26	478,000	0.00625
400	50	4.20	598,000	0.00743
400	60	6.65	718,000	0.00810
400	70	9.10	838,000	0.00820
400	80	11.90	958,000	0.00822
400	90	14.5	1,079,000	0.00791
400	100	17.2	1,196,000	0.00763
400	120	22.5	1,435,000	0.00691
1,000	25	0.67	298,000	0.00557
1,000	30	0.93	358,000	0.00538
1,000	40	1.78	478,000	0.00578
1,000	50	3.25	597,000	0.00677
1,000	60	5.20	717,000	0.00751
1,000	70	7.20	837,000	0.00765
1,000	80	9.70	955,000	0.00789

(1)	(2)	(3)	(4)	(5)
1,000	90	12.00	1,074,000	0.00771
1,000	100	14.30	1,193,000	0.00746
1,000	120	19.10	1,432,000	0.00690
2,000	25	0.6	298,000	0.00533
2,000	30	0.83	357,000	0.00510
2,000	40	1.52	477,000	0.00525
2,000	50	2.74	597,000	0.00606
2,000	60	4.32	716,000	0.00663
2,000	70	6.2	835,000	0.00700
2,000	80	7.3	954,000	0.00631
2,000	90	10.5	1,073,000	0.00718
2,000	100	12.8	1,192,000	0.00709
2,000	120	17.1	1,431,000	0.00658
4,000	25	0.54	298,000	0.00492
4,000	30	0.75	356,000	0.00475
4,000	40	1.31	477,000	0.00467
4,000	50	2.25	596,000	0.00514
4,000	60	3.62	716,000	0.00574
4,000	70	5.30	834,000	0.00617
4,000	80	7.20	953,000	0.00641
4,000	90	9.20	1,073,000	0.00648
4,000	100	11.4	1,192,000	0.00651
4,000	120	15.2	1,431,000	0.00602
10,000	25	0.48	298,000	0.00451
10,000	30	0.67	356,000	0.00433
10,000	40	1.14	477,000	0.00415

(1)	(2)	(3)	(4)	(5)
10,000	50	1.80	596,000	0.00419
10,000	60	2.91	716,000	0.00471
10,000	70	4.4	833,000	0.00523
10,000	80	6.0	953,000	0.00545
10,000	90	7.8	1,073,000	0.00561
10,000	100	9.7	1,191,000	0.00565
10,000	120	13.2	1,430,000	0.00534
20,000	25	0.46	298,000	0.00432
20,000	30	0.64	356,000	0.00417
20,000	40	1.04	477,000	0.00381
20,000	50	1.58	596,000	0.00371
20,000	60	2.48	716,000	0.00404
20,000	70	3.82	833,000	0.00457
20,000	80	5.25	953,000	0.00482
20,000	90	7.00	1,073,000	0.00507
20,000	100	8.8	1,191,000	0.00516
20,000	120	12.0	1,430,000	0.00489
40,000	25	0.45	298,000	0.00414
40,000	30	0.61	356,000	0.00401
40,000	40	0.99	477,000	0.00363
40,000	50	1.48	596,000	0.00348
40,000	60	2.20	716,000	0.00359
40,000	70	3.32	833,000	0.00398
40,000	80	4.54	953,000	0.00417
40,000	90	6.20	1,073,000	0.00450
40,000	100	7.90	1,191,000	0.00464
40,000	120	10.90	1,430,000	0.00445

(1)	(2)	(3)	(4)	(5)
100,000	25	0.42	290,000	0.00403
100,000	30	0.58	356,000	0.00379
100,000	40	0.95	477,000	0.00350
100,000	50	1.42	596,000	0.00334
100,000	60	2.04	716,000	0.00334
100,000	70	2.94	833,000	0.00353
100,000	80	4.00	953,000	0.00368
100,000	90	5.40	1,073,000	0.00392
100,000	100	7.0	1,191,000	0.00412
100,000	120	9.8	1,430,000	0.00402
1,000,000	25	0.40	298,000	0.00377
1,000,000	30	0.55	356,000	0.00364
1,000,000	40	0.94	477,000	0.00344
1,000,000	50	1.41	596,000	0.00332
1,000,000	60	1.96	716,000	0.00321
1,000,000	70	2.65	833,000	0.00319
1,000,000	80	3.48	953,000	0.00321
1,000,000	90	4.32	1,073,000	0.00314
1,000,000	100	5.00	1,191,000	0.00294
1,000,000	120	8.20	1,430,000	0.00336

SECTION B-9
CALCULATION OF DATA

1. Gas Flow Rate

The orifice flow equation may be written in the form

$$Q_g = \frac{C'}{3600} \sqrt{h_w P_f} \quad (17)$$

where Q_g = gas flow rate in standard cubic feet per second (S.C.F.S.) at 14.4 psia and 60°F.

h_w = differential pressure in inches of water.

P_f = static pressure in p.s.i.a.

$C' = F_b \times F_r \times Y \times F_{pb} \times F_{tb} \times F_{tf} \times F_g \times F_{pv} \times F_m.$

The values of all the factors F_b , F_r , etc. are obtained from the tables in Section V of American Gas Association, Gas Measurement Committee Report No. 3.

2. Gas Density at the Mid-point

The gas law may be written in the form

$$\rho_g = \frac{29 G P_3}{Z R T} \quad (18)$$

where ρ_g = density of the gas at the mid-point
 temperature and pressure, lbs. per ft.³
 G = gravity of the gas (Air = 1.0)
 P_3 = mid-point pressure, p.s.i.a.
 T = average gas temperature, °R.
 R = gas constant = 10.73
 Z = compressibility factor

3. Superficial Gas Velocity at the Mid-Point

The continuity equation may be written in the form

$$V_g = \frac{\rho_g^* Q_g}{\rho_g A} \quad (19)$$

where V_g = superficial gas velocity, ft. per sec.

ρ_g^* = gas density at standard conditions

$$= \frac{29 G (14.4)}{1 \times 10.73 \times 520}$$

$$= 0.0488 \text{ lbs. per ft.}^3$$

Q_g, ρ_g as previously defined

A = transverse internal pipe area, ft.²

Equation (19) reduces to

$$V_g = 8.133 \frac{Q_g}{\rho_g} \text{ for the one-inch pipe} \quad (20)$$

$$V_g = 2.098 \frac{Q_g}{\rho_g} \text{ for the two-inch pipe} \quad (21)$$

4. Water Rate

The orifice flow equation for incompressible fluids may be written in the form

$$Q_w = C'' \sqrt{h_w} \quad (22)$$

C'' = orifice constant

h_w = differential pressure

= (Instrument Reading)² x 8

The flow rates were directly obtained from the orifice calibration curves, Figure C-1.

5. Superficial Water Velocity

$$V_w = \frac{Q_w}{A} \quad (23)$$

where V_w = superficial water velocity, ft. per sec.

6. Reynolds number Based on Mixture Properties

$$Re_m = D \left[\frac{\rho_g V_g}{\mu_g} + \frac{\rho_w V_w}{\mu_w} \right] \quad (14)$$

where Re_m = Reynolds number based on mixture properties.

μ_g = gas viscosity, $\frac{\text{lb.}}{\text{ft. sec.}}$

= 0.679×10^{-5}

μ_w = water viscosity, $\frac{\text{lb.}}{\text{ft. sec.}}$

= 0.672×10^{-3}

ρ_g = gas density at the mid-point, lbs. per ft.³ = 0.47.

ρ_w = water density at the mid-point, lbs.
per ft.³ = 62.43.

D = internal pipe diameter, ft. = .0874 and
.1722.

V_g, V_w as previously defined

7. Friction Factor based on input Mixture Properties

$$f_{tpm} = \frac{\left(\frac{dP}{dL}\right) g_c D}{2 (V_g + V_w)^2 \rho_m} \quad (13)$$

where f_{tpm} = friction factor based on mixture
properties.

$\left(\frac{dP}{dL}\right)$ = pressure gradient at the mid-point.

$$g_c = 32.1740 \frac{lb_m}{lb_f} \frac{ft.}{sec^2}$$

ρ_m = mixture density

$$= \frac{\rho_g V_g + \rho_w V_w}{V_g + V_w}$$

$D, V_g, V_w, \rho_g, \rho_w$ as previously defined.

8. Reynolds Number based on Gas Properties

$$Re_g = \frac{D \rho_g V_g}{\mu_g}$$

where Re_g = Reynolds number based on gas properties
at the mid-point.

The equation reduces to

$$Re_g = 12878 \rho_g V_g \text{ for the one-inch pipe} \quad (24)$$

$$Re_g = 25377 \rho_g V_g \text{ for the two-inch pipe} \quad (25)$$

9. Friction Factor based on Gas Properties

$$f_{tpg} = \frac{\left(\frac{dP}{dL}\right) g_c D}{2 V_g^2 \rho_g} \quad (26)$$

where f_{tpg} = friction factor based on gas properties.

The equation reduces to

$$f_{tpg} = 1.407 \left(\frac{dP}{dL}\right) \frac{1}{\rho_g} \frac{1}{V_g^2} \quad (27)$$

for the one-inch pipe

$$f_{tpg} = 2.777 \left(\frac{dP}{dL}\right) \frac{1}{\rho_g} \frac{1}{V_g^2} \quad (28)$$

for the two-inch pipe

APPENDIX C
CALIBRATION OF THE EQUIPMENT

- C-1 Gas Orifice Meter
- C-2 Pneumatic Recorders
- C-3 Pneumatic D/P Cells
- C-4 Orifice Calibration for the D/P Cell
- C-5 Electrical D/P Cell and Recorder

APPENDIX C

CALIBRATION OF THE EQUIPMENT

C-1

Gas Orifice Meter:

The static pressure element on the gas flow recorder was calibrated against a dead-weight pressure gauge. No correction to the chart reading was necessary over the range of interest. The differential element was calibrated against a mercury manometer and no correction was necessary to the chart reading.

Individual orifices were not calibrated. The calibration data of American Gas Association, Gas Measurement Committee Report No. 3, were used for all flow calculations. A few spot checks were, however, made on two of the orifices by the use of a precalibrated critical flow prover. In all cases the gas measurement by the orifice meter was within 1% of the measurement by the critical flow prover.

C-2

Pneumatic Recorders:

Pneumatic recorders were used to record the pressure drop in the integral orifice D/P cell for water measurement,

mid-point pressures in the two-inch and the one-inch test sections, and the pressure drop in the two-inch test section. The recorders were calibrated against a test gauge by supplying a pressure of 3 to 15 psig to the recorder.

C-3

Pneumatic D/P Cells:

The pressure across the diaphragm of a D/P cell was measured on a manometer and the output of the D/P cell was recorded on a precalibrated recorder. The range of all pneumatic D/P cells was checked in this manner, including the integral orifice D/P cell for which the orifice was removed for range calibration.

C-4

Orifice Calibration for the D/P Cell:

Orifices for the integral orifice D/P cells were calibrated by collecting the water for certain periods of time and weighing it. The calibration data for 0.25, 0.0595, 0.034, 0.0995 and 0.02 inch orifices is plotted in Figure C-1 as instrument (recorder) reading versus water rate in cm^3/sec . The recorder had a square root chart and a range of 0-800 inches of water.

C-5

Electrical D/P Cell and Recorder:

The electrical recorder and the electrical D/P cell were checked in the same manner as the pneumatic instruments. They were both found to be more accurate than the pneumatic instruments.

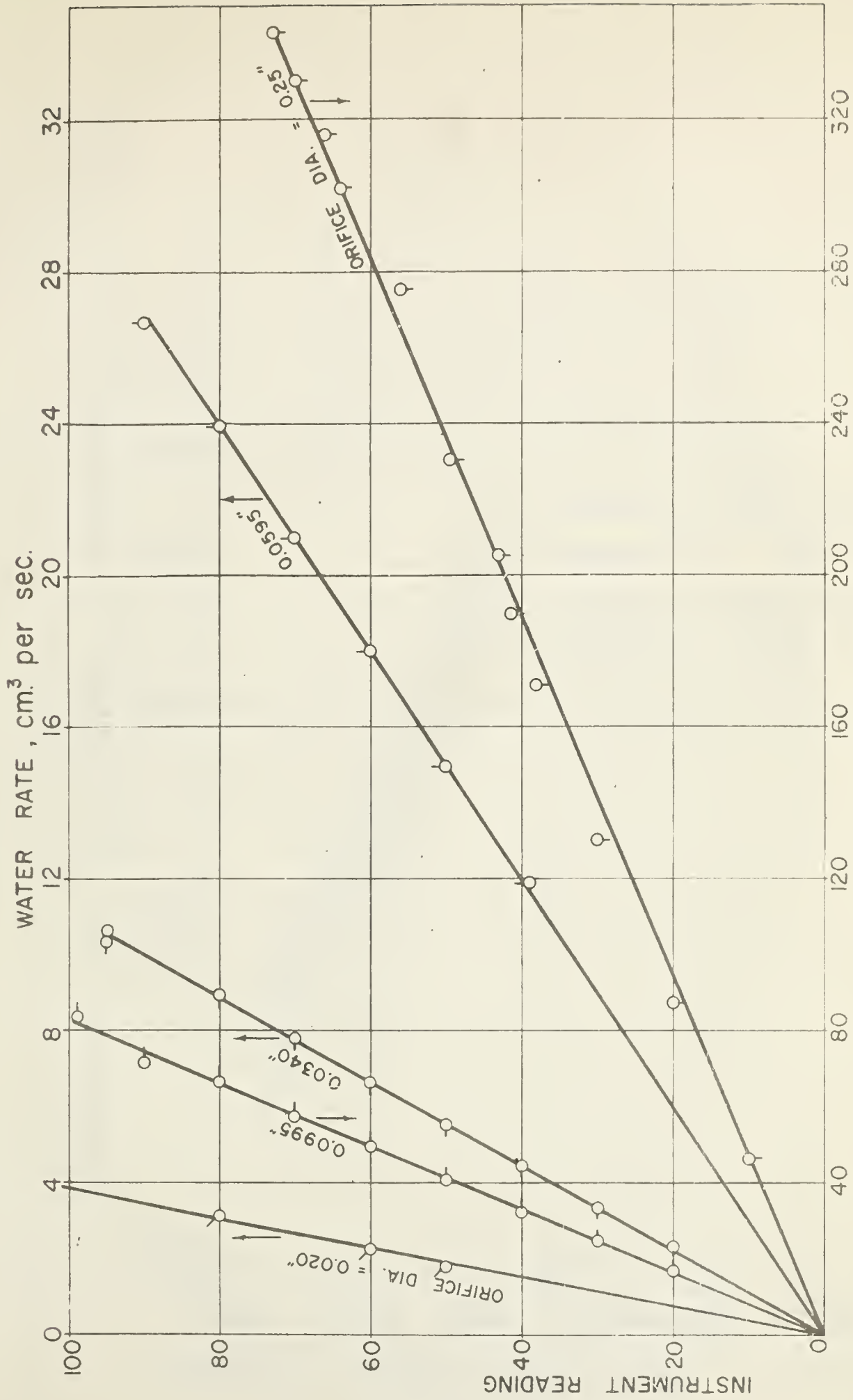
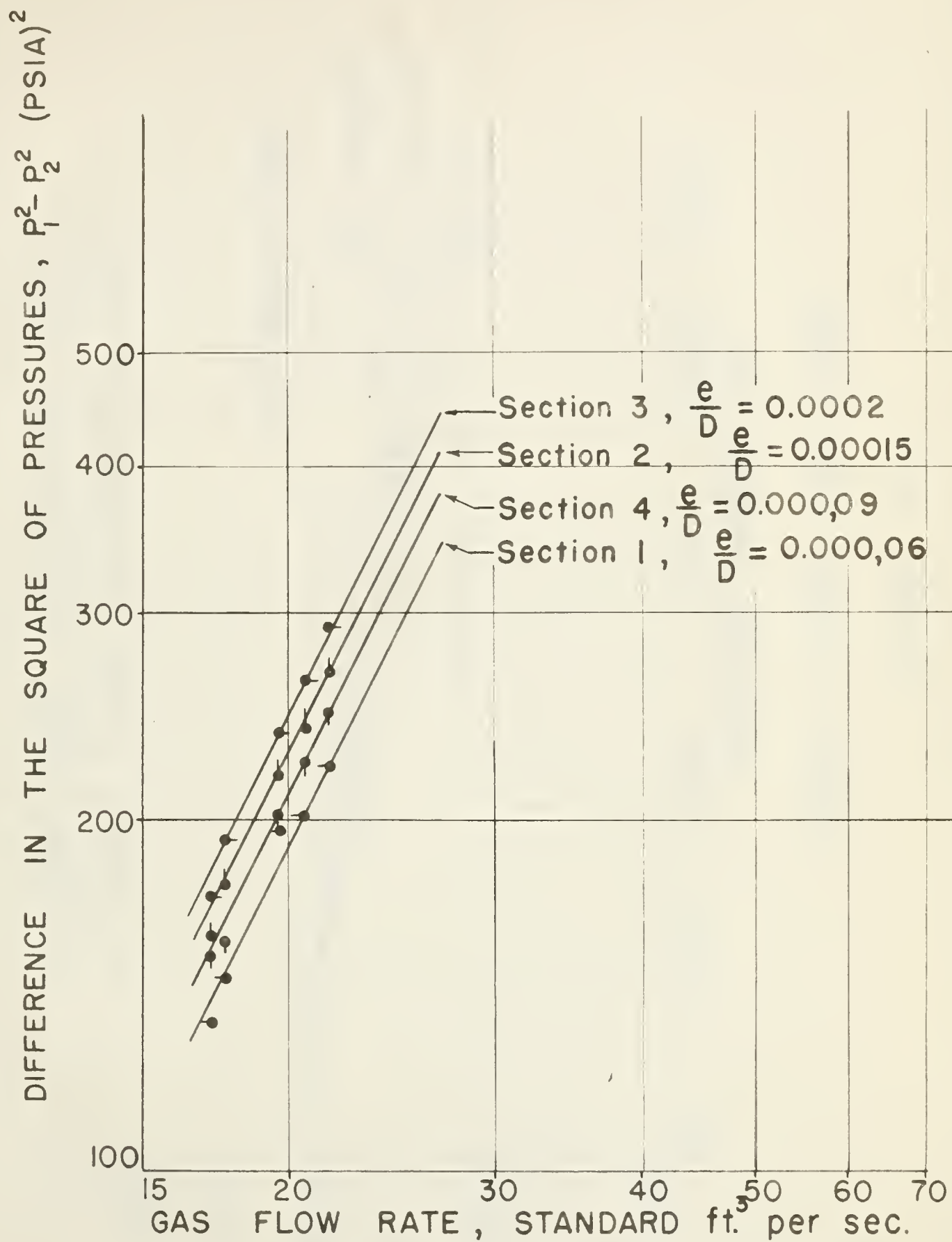
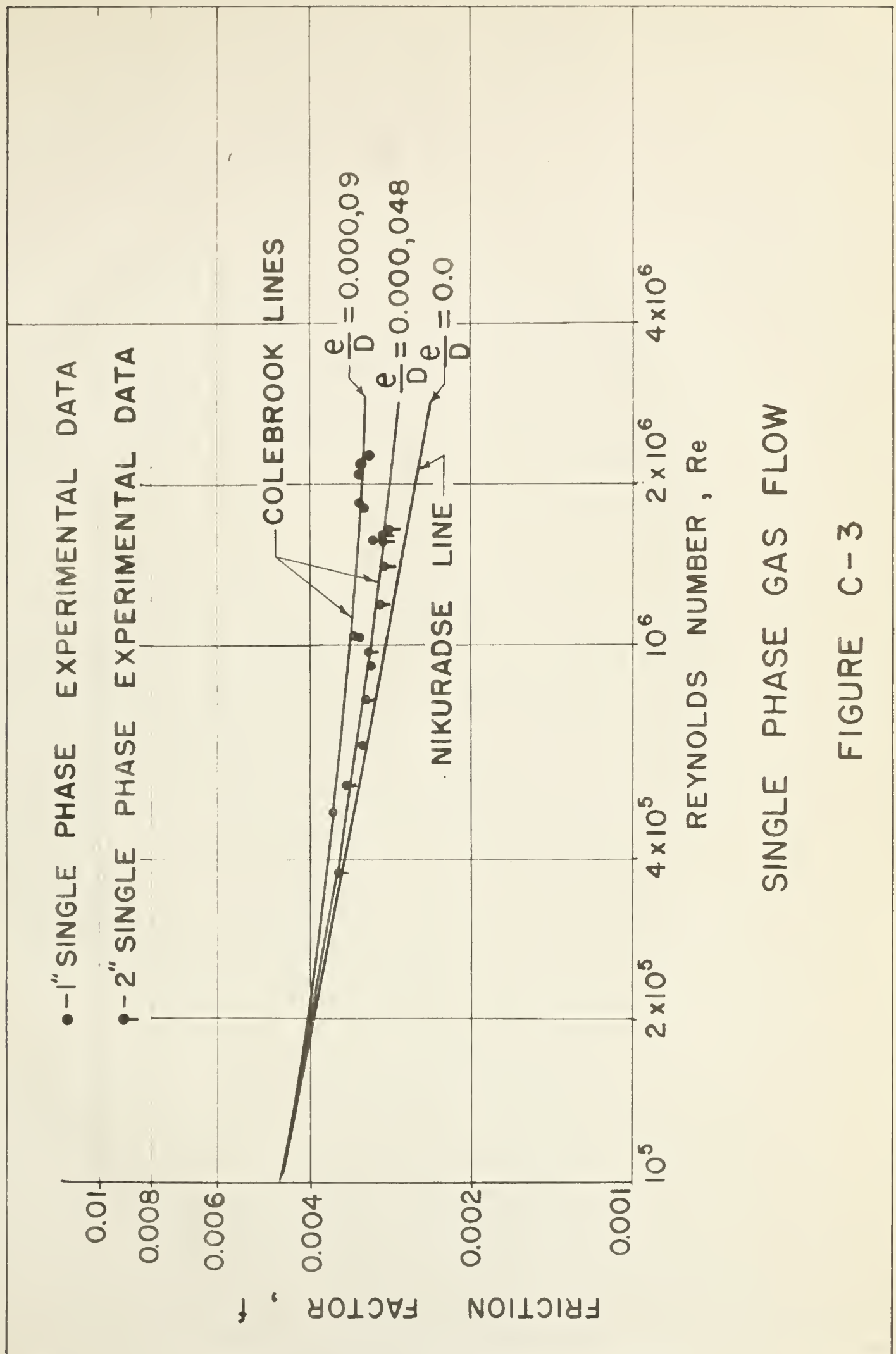


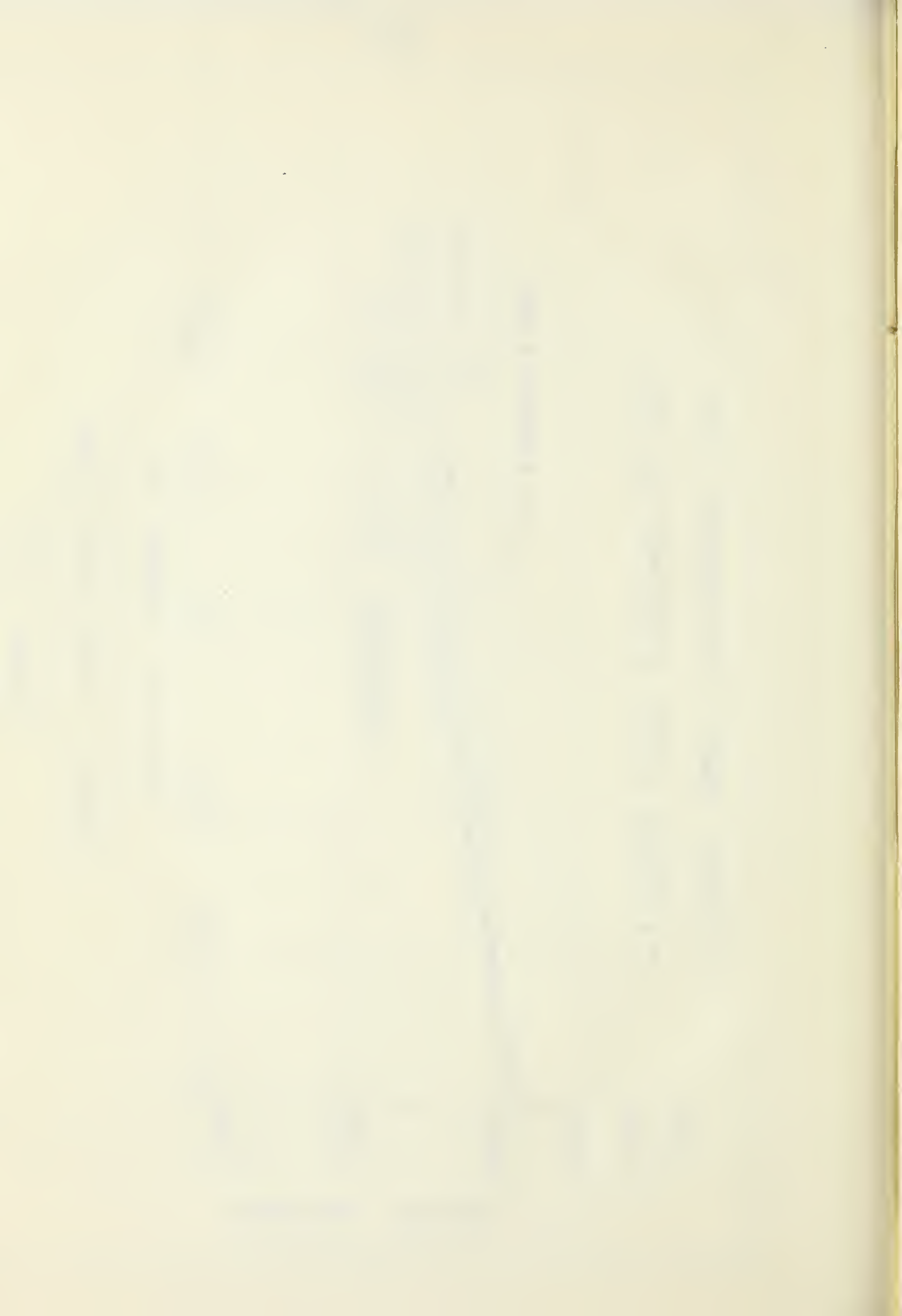
FIGURE C-1, CALIBRATION OF WATER D/p CELL ORIFICES

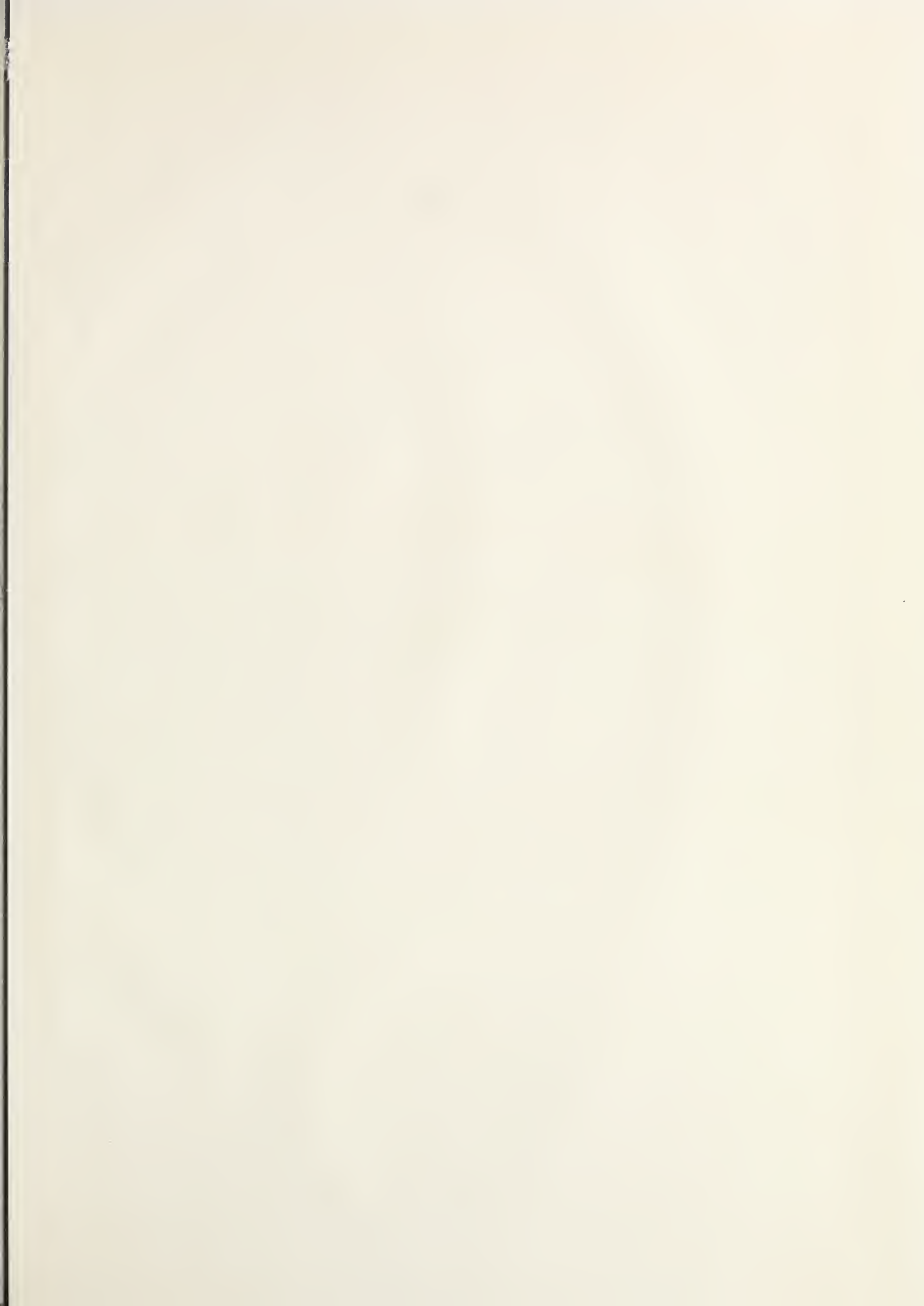


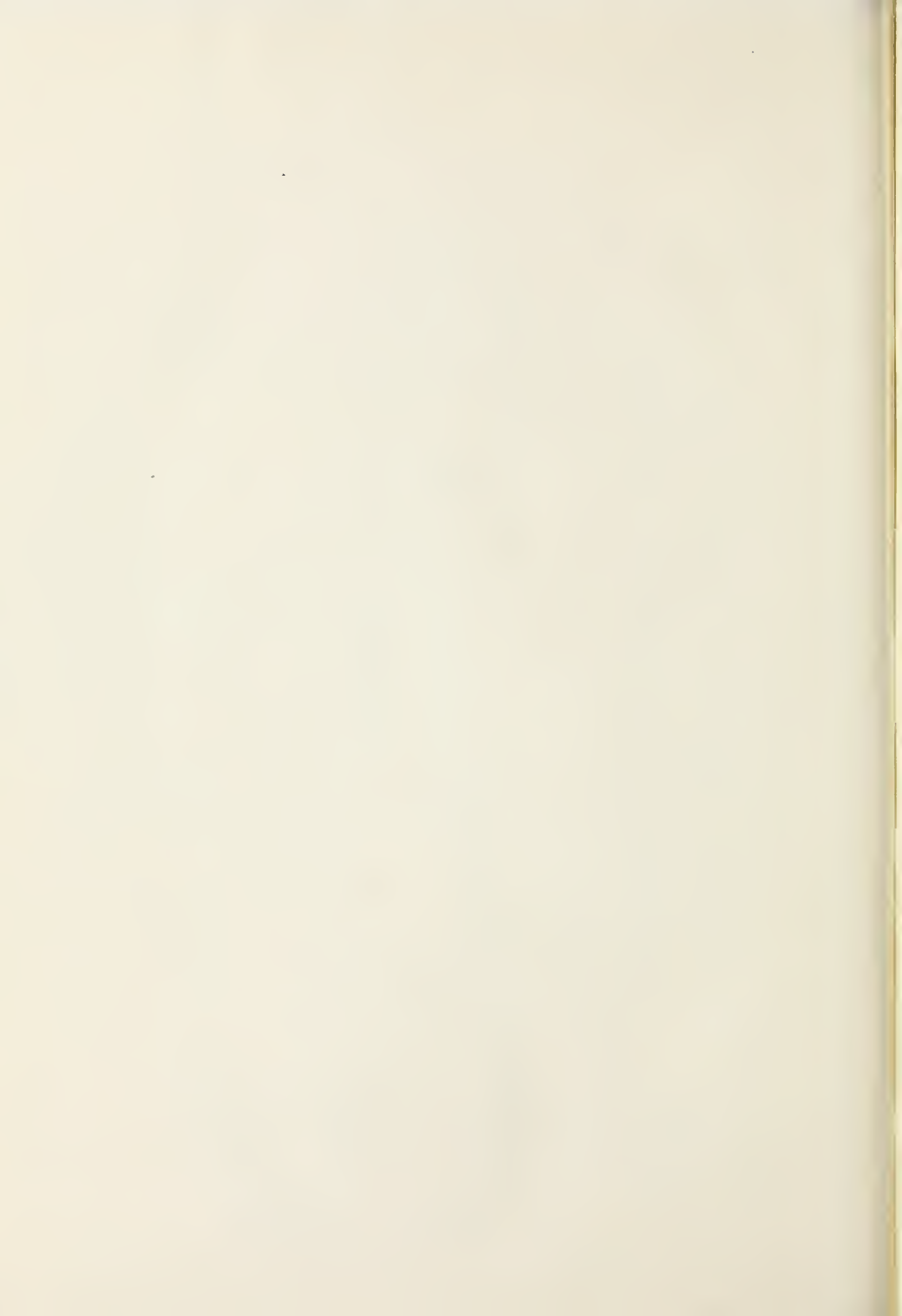
SINGLE PHASE GAS FLOW — 1" PIPE

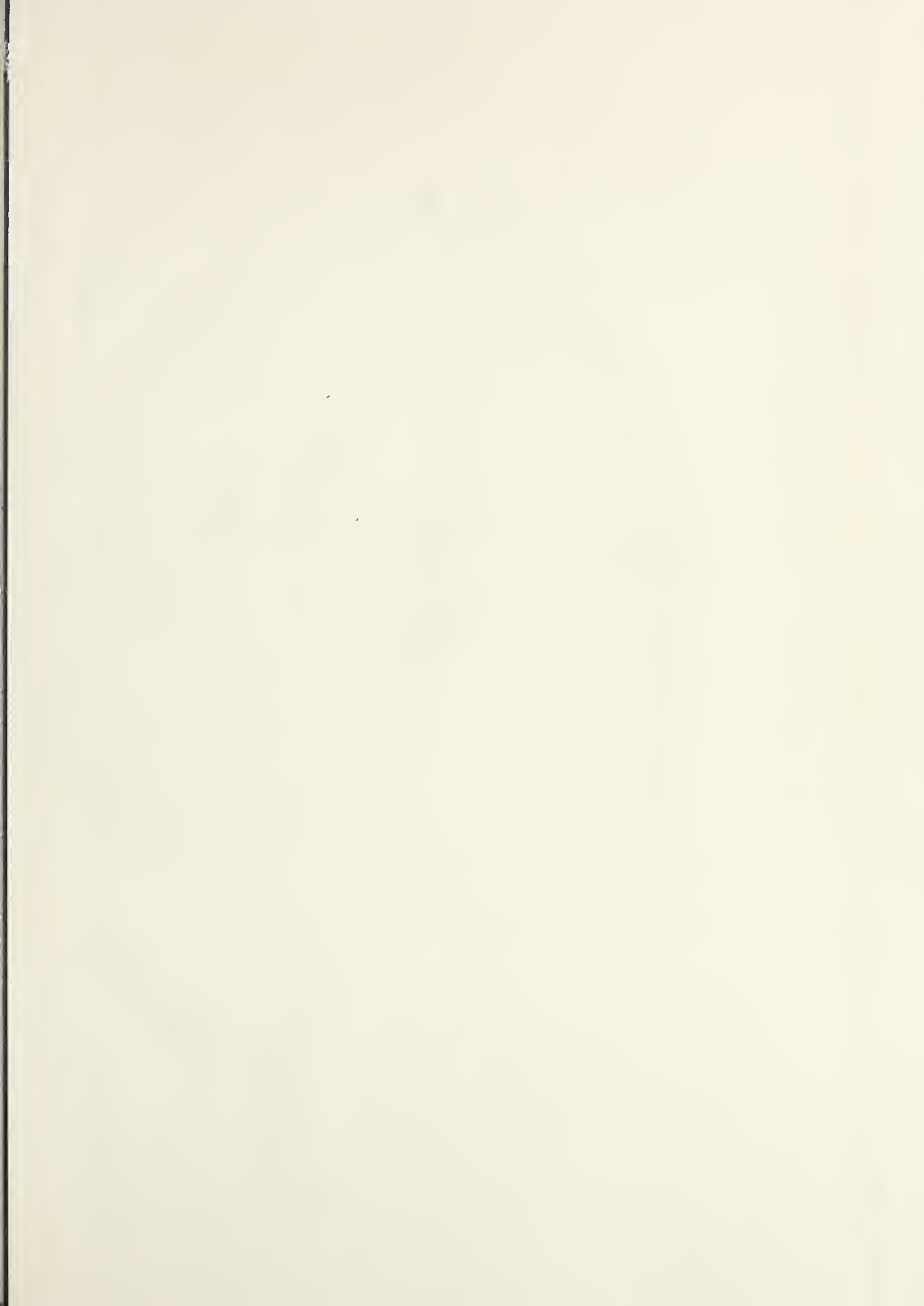
FIGURE C-2













B29790